



POLITECNICO DI TORINO

DIPARTIMENTO DI INGEGNERIA MECCANICA E AEROSPAZIALE
(DIMEAS)

Master's Degree in Biomedical Engineering

**Exploring the use of Mitsui's flexible
optical sensor as a means to monitor
knee flexion-extension angular
displacement during ambulation**

Supervisor
Prof. Danilo DEMARCHI

Candidate
Monica MURA

TORINO, March 2020

Abstract

A branch of the wearable sensor research focuses on monitoring the human body joints movements to prevent injuries due to musculoskeletal disorders. Different types of sensors and technologies are used as a core of a smart joint monitoring system, one of these are optical fiber sensors.

Optical fiber sensors are used to monitor joint angles with the main advantages to have a high resolution, a light-weight and to be flexible. For these reasons, they can be integrated into stretchable skin-tight fabrics to create a wearable joint monitoring system.

In this thesis, a prototype developed by Mitsui Chemicals has been tested. The prototype is composed of a sleeve with five integrated optical fiber sensors placed medially, laterally, inside-medially and inside-laterally than the knee and above the patella. The purpose of this work is to evaluate the performance of the Mitsui's optical fiber sensors in predicting knee flexion-extension angular displacement.

The first step of the study is the creation of a dataset to train a machine learning algorithm.

Twenty healthy participants have been selected to perform the data collection. They have been requested to wear the prototype during ambulation on a treadmill at different speeds while the voltage outputs and the knee angles have been recorded using the Vicon Motion Capture system. Three sizes of the prototype have been used during the data collection: for each subject, the size with a closer fit that won't create discomfort to the subject has been chosen.

An outlier detection algorithm has been developed to analyze the voltage outputs to find possible outliers due to a not optimal fit of the sleeve. This algorithm recognizes as outliers signals with a low correlation value and large amplitude respect the other signals of the sensor with the same position in the sleeve prototype.

The outliers are subsequently removed from the dataset by a custom replacement algorithm. Demonstrating the high correlation among medially, laterally and patella sensors, and inside-medially and inside-laterally sensors, it's possible to replace outliers of one sensor with the data of the same correlated sensor.

Two different types of models to predict the knee angle are used: one model without memory, the Random forest (RF), and one model with memory, the Long short-term memory (LSTM). The models are applied to the dataset with a leave-one-subject-out (LOSO) cross-validation (CV) approach and their performances are evaluated in terms of root-mean-squared error (RMSE). The overall RMSE obtained for the RF model is 5.22° and the LSTM model is 4.56° . The average error is similar, however, the LSTM performs better than the Random Forest in 80% of the subjects.

Contents

Abstract	IV
List of Tables	VII
List of Figures	VIII
Acronyms	X
1 Introduction	1
1.1 Overview of musculoskeletal system	1
1.1.1 Musculoskeletal disorders	4
1.2 Overview of knee joint	6
1.2.1 Knee joint disorders	8
2 State of the Art	10
2.1 Joint monitoring	10
2.1.1 Optical fiber sensors	13
2.1.2 Vicon motion capture system	16
2.1.3 Random forest	17
2.1.4 Long short-term memory	19
2.2 Mitsui's prototype	21
3 Materials and Methods	24
3.1 Data collection	24
3.2 Data pre-processing	28
3.3 Outlier detection algorithm	31
3.3.1 Correlation analysis	31
3.3.2 Amplitude analysis	32
3.4 Outlier replacement algorithm	34
3.5 Machine learning algorithm	36

3.5.1	Random Forest	37
3.5.2	Long short-term memory	37
4	Results	39
4.1	Outlier detection algorithm	39
4.2	Outlier replacement algorithm	41
4.3	Machine learning algorithm	41
4.4	Discussion	42
5	Conclusions	49
	Bibliography	51

List of Tables

3.1	Subjects involved in data collection	25
3.2	Voltage signals of the dataset divided by channels and by speed . .	31
4.1	Replacements across subjects	41
4.2	RMSE values results	41

List of Figures

1.1	Musculoskeletal system	1
1.2	Synovial joint	3
1.3	Types of synovial joint	3
1.4	Osteoporosis	4
1.5	Sarcopenia	5
1.6	Arthritis	5
1.7	Main components of knee joint	7
1.8	Types of knee joint arthritis	9
1.9	Knee joint osteoarthritis	9
2.1	Types of joint movements	12
2.2	Flow diagram of a generic joint monitoring system	13
2.3	Schematic of an optical fiber	14
2.4	Knee monitoring using optical fiber	15
2.5	An Optical Fiber Bragg grating structure	15
2.6	Vicon Nexus 2.0 main panel	16
2.7	Decision Tree generic structure	17
2.8	Random Forest generic structure	19
2.9	Long Short-Term Memory generic block structure	20
2.10	Long Short-Term Memory generic structure	21
2.11	Mitsui Chemicals prototype	22
2.12	Mitsui box	22
2.13	Voltage output behaviour of the five Mitsui sensors	23
3.1	Lower limb marker set positioning	26
3.2	Setup of trials with Mitsui prototype	27
3.3	Data collection output	28
3.4	Results of low-pass filtering	29
3.5	Results of high-pass filtering	29
3.6	Results of normalization	30
3.7	Correlation analysis output	32

3.8	Normal distribution	33
3.9	Amplitude analysis output	33
3.10	Correlation coefficients extraction	34
3.11	Correlation coefficients of the five channels	35
3.12	Outliers replacement	36
3.13	LSTM network designed	38
4.1	Outliers across channels	39
4.2	Outliers across speeds	40
4.3	Outliers across subjects	40
4.4	Correlation analysis results	44
4.5	Amplitude analysis results	45
4.6	Total outliers detected	46
4.7	Outliers replacement results	47
4.8	Machine learning models results	48

Acronyms

ACL anterior cruciate ligament.

CC correlation coefficient.

CV cross-validation.

IMU inertial measurement unit.

LOSO leave-one-subject-out.

LSTM Long short-term memory.

PCL posterior cruciate ligament.

RF Random forest.

RMSE root-mean-squared error.

ROM range of motion.

SD standard deviation.

SS self-selected.

Chapter 1

Introduction

1.1 Overview of musculoskeletal system

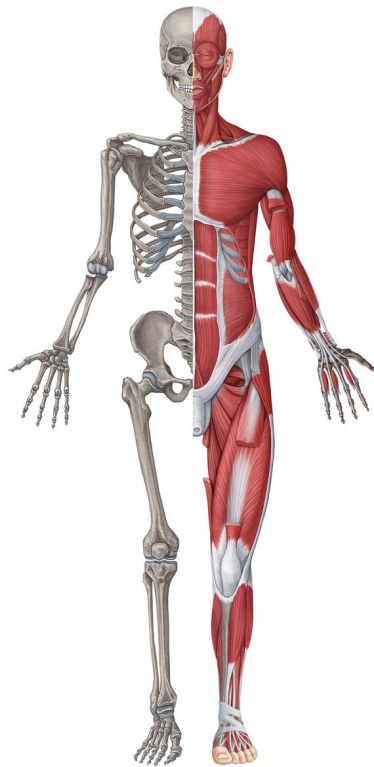


Figure 1.1: Musculoskeletal system. [1]

The musculoskeletal system (Figure 1.1) is an organ system with the primary functions of supporting, providing stability and mobility to the body [2].

It is primarily made up of [3]:

- **Connective tissue:** includes white fibrous tissue, this one has high tensile strength and forms ligaments and tendons. The first ones pass from one bone to another in the region of joints, connecting the bones and limiting joint movements, the second ones attaching muscles to the bones;
- **Skeletal tissues:** has the main functions of give support to the body and to absorb shock. It comprises cartilages and bones. The first ones cover the end of bones to cushion impacts and to reduce friction inside a joint, the second ones give stability to the body;
- **Muscular tissue:** is responsible for the generation of movement, giving support to the body and stability to the joints. It is composed of skeletal muscles, these are connected directly or through tendon to the bones and with their contraction, they move bone and generate joint motion;
- **Joints:** are the locations where bones come together and movement occurs, they permit and limit specific movements. Based on the structure and the function of the joint they allow different types of movements and can be categorized into three classes: fibrous, cartilaginous and synovial, with increasing mobility from the first one to the third one. Synovial joints (Figure 1.2) are a class of freely mobile joints and the majority of the joints of the limbs belong to this class. In this type of joint the articular surfaces of the bones are covered by articular cartilage to enable them to move on each other with minimum friction and to protect them from impact. Surrounding the joint there is a connective tissue sleeve, the articular capsule, that held the bones together. Lining the internal surface of the capsule there is the synovial membrane, that covers all non-articular surfaces within the capsule. This membrane secret synovial fluid into a space called joint cavity to lubricate and nourishing the articular cartilage. There is a large number of synovial joints inside the body and they can be subdivided into six groups based on their articular surfaces and the movements possible at the joint (Figure 1.3). In particular, a hinge joint is a type of synovial joint that allows movement about one axis only, consequently the two articular surfaces fitting is usually good and the joint is supported by strong collateral ligaments. One example of a hinge joint is the knee joint. More precisely, it is a synovial modified hinge joint because due to a poor fit of the articular surfaces it permits movement also about a second axis.

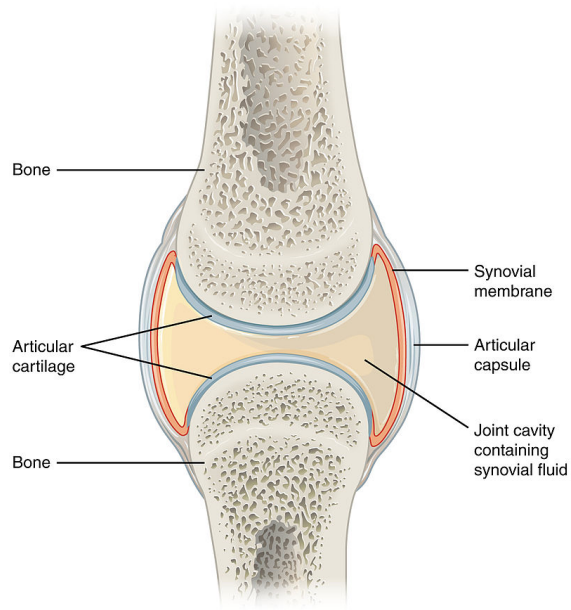


Figure 1.2: Synovial joint. [4]

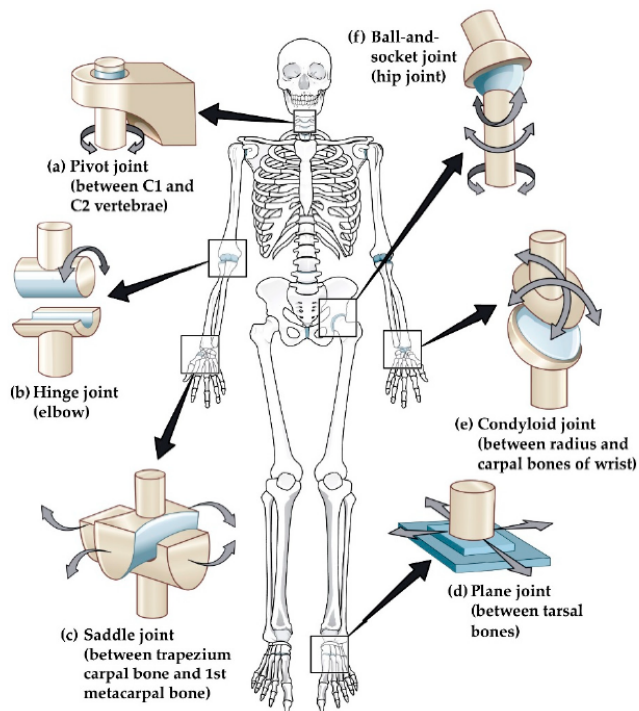


Figure 1.3: Types of synovial joint. [4]

1.1.1 Musculoskeletal disorders

Musculoskeletal disorders are clinical conditions that affect the components of the musculoskeletal system and may range from minor physical disabilities to disease. Examples of musculoskeletal disorder that involve the three main components of the musculoskeletal system are [1]:

- Osteoporosis: is a condition that affects the bones. They become fragile and brittle leading to a higher risk of fractures than in normal bone. In this case, even a minor bump or accident can cause serious fractures (Figure 1.4);
- Sarcopenia: is a condition that affects skeletal muscles. Is characterized by progressive and generalized loss of muscle mass and muscle strength with the risk of an adverse outcome as physical disability and poor quality of life (Figure 1.5);
- Arthritis: groups of conditions affecting the joints. The joint tissue starts to degenerate, resulting in pain, stiffness, and loss of mobility. This condition can affect different parts of the joint and nearly every joint in the body (Figure 1.6).

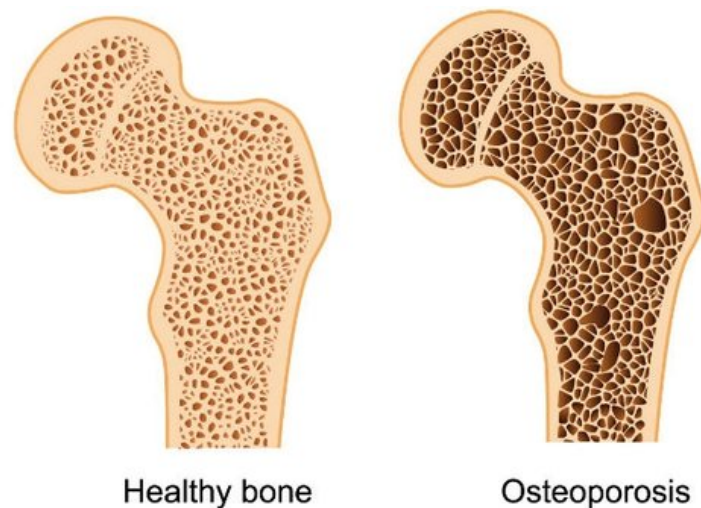


Figure 1.4: Osteoporosis.



Figure 1.5: Sarcopenia.

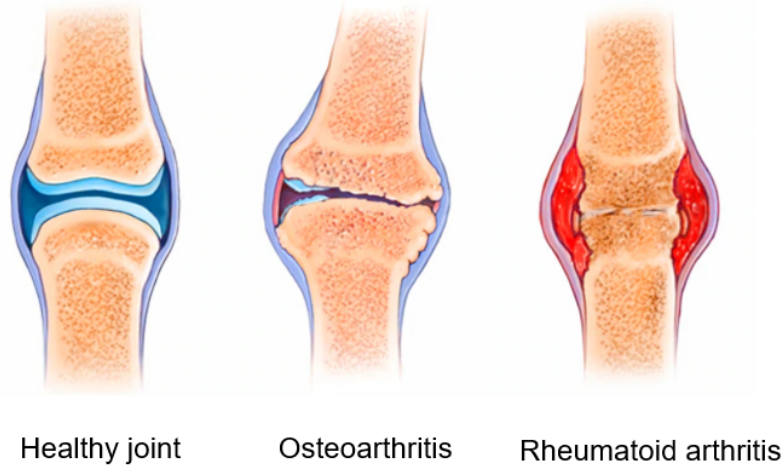


Figure 1.6: Arthritis.

Musculoskeletal disorders rank fourth in total global death and disability burden and are the top-ranked common cause of disability among older adults. Subjects with these conditions have limitation in mobility that causes reduced ability to work and participate in social life, with mental consequences for the subject and relevant economic consequences on the society. The cost of treatment and healthcare services are a major social and financial burden on society. To limit the impact of this disorder, primary prevention, early detection and effective interventions for persons at risk of musculoskeletal health issues are crucial. [4]

1.2 Overview of knee joint

The knee joint is the largest and one of the most complex joints in the body. Its complexity is due to an optimal interaction of bony structures such as femur, tibia, patella, and fibula, as well as its ligament, muscles, and tendons. Generally, each function of the knee is the result of the teamwork of several anatomical structures together. It carries a large portion of the body weight and allows a wide flexion-extension and a small internal-external rotation. Since it permits mainly a movement in one axis but also small mobility in a second axis it is considered a modified hinge joint. [5]

It is composed of three articulations: medial tibiofemoral, lateral tibiofemoral and patellofemoral. The first two linking the femur with the tibia, the second one brings together the patella and the femur. The main components of the knee joint are the following (Figure 1.7) [6].

- **Femur (thigh bone):** bone that run from the knee to the hip. Its end is cover by articular cartilage and the round knobs on it are called condyles;
- **Tibia (shin bone):** bone that run from the ankle to the knee. Its top is composed of two plateau covered by articular cartilage. Over them there are two crescent-shaped shock-absorbing cartilages called menisci;
- **Patella (kneecap):** semi-flat and triangular bone that can move as the knee bends. Its primary functions are to increase the force generated by the quadriceps muscle during knee extension and protect the knee joint from trauma. The patella fits inside the groove formed between the two femoral condyles;
- **Fibula:** thin bone that run along side the tibia from the ankle to the knee. It give small support to the tibia in carrying the weight and serves as an attachment for the biceps femoris and the lateral collateral ligament.
- **Medial (or tibial) collateral ligament and lateral (or fibular) collateral ligament:** both attache the femur and the tibia, the first one medially and the second one laterally, and limit sideways motion of the knee joint;
- **Anterior cruciate ligament (ACL) and posterior cruciate ligament (PCL):** both attache the femur and the tibia, limit some rotation and sideways motion of the knee joint and are positioned deep inside the knee one in front each other. ACL limit forward motion of the tibia relative to the femur, vice-versa PCL limits backward motion of the tibia relative the femur;

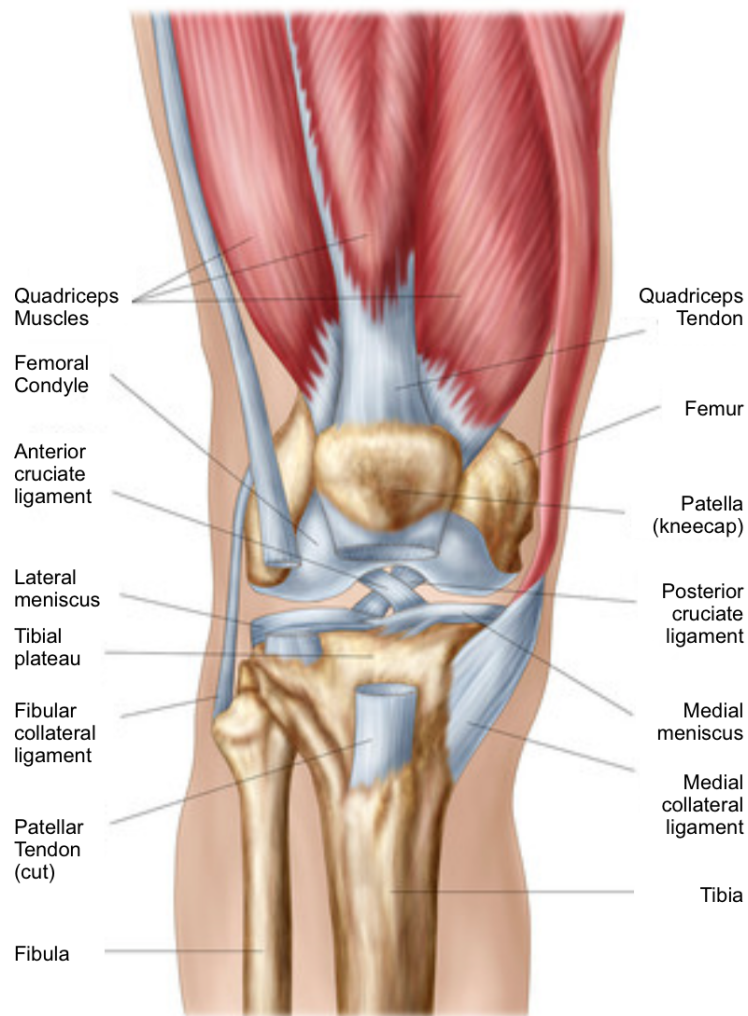


Figure 1.7: Main components of knee joint (front view).

- **Patellar ligament (or tendon):** attaches the patella to the tibia. It is more a continuation of the quadriceps tendon than a ligament;
- **Joint capsule:** fibrous structure that surround the knee joint and inside it, there is the synovial membrane that secretes synovial fluid to facilitate the movement of the joint.
- **Medial meniscus and lateral meniscus:** two crescent shaped structure made of fibrocartilage wich make them strong, rubbery and able to add additional stability to the knee;

- **Quadriceps and hamstrings:** two groups of muscles positioned around the knee that help to keep the knee stable and allow knee joint motion. Quadriceps are responsible for the knee extension and hamstrings are responsible for the knee flexion;
- **Quadriceps tendon:** situated on the front of the knee and connects the quadriceps muscles of the thigh to the tibia via the patella and patellar ligament. It gives the strength necessary to straighten the knee.

The pair of collateral ligament and the pair of cruciate ligament, working together are the most important structures in controlling the stability of the knee.

1.2.1 Knee joint disorders

As the knee joint is composed of many structures, numerous problems can involve him. These can be injury or pathological conditions. Regarding the second case, the most common disease affecting the knee joint is arthritis. The major type of arthritis that affects the knee is [7] (Figure 1.8):

- **Osteoarthritis:** is the most common arthritis in the knee. It is a type of arthritis that involves the articular cartilage presents at the end of the bones inside the joint. It consists in wear and tear of the articular cartilage due to aging or to previous injury that accelerates the degenerative process. This loss of cartilage protection results in an area of exposed bone and in bone-to-bone rubbing that creates bone spurs around the joint. (Figure 1.9)
- **Rheumatoid arthritis:** is an autoimmune disease where the immune system produces antibodies against joint tissue. This results in inflammation and thickening of the joint capsule because the synovial membrane starts to swelling.

In general, the primary symptoms of arthritis are discomfort, swelling, stiffness, and pain. With the progress of the disease, the pain can interfere with simple daily activities like walking or climbing the stairs, limiting the mobility of the subject.

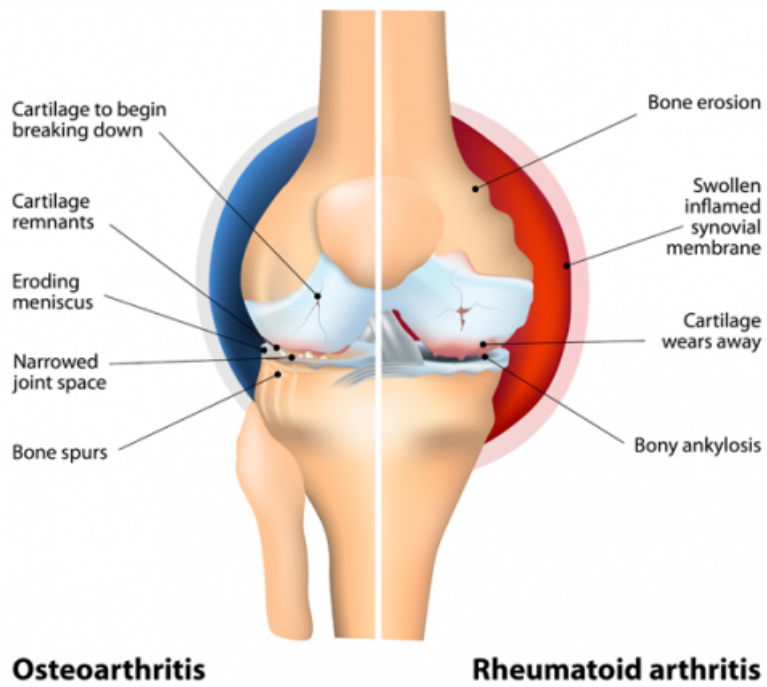


Figure 1.8: Types of knee joint arthritis

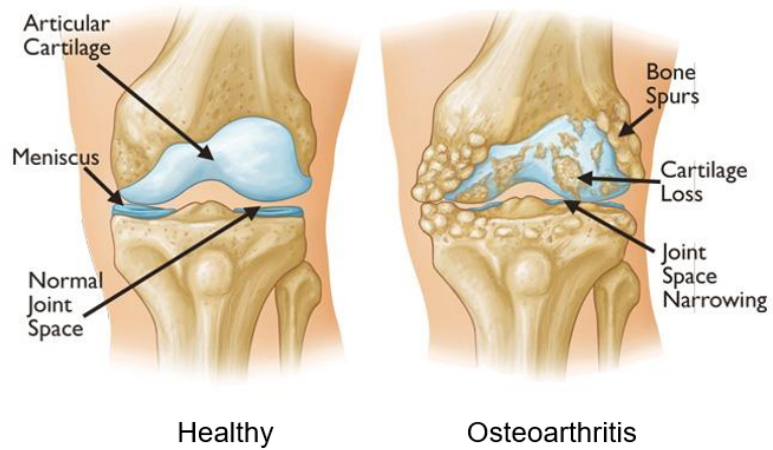


Figure 1.9: Knee joint osteoarthritis. [7]

Chapter 2

State of the Art

2.1 Joint monitoring

The worst outcome of musculoskeletal disorders is the loss of mobility that prevents subjects to be independent, to work and to be an active part of society. For this reason, prevention with monitoring of musculoskeletal parameters in subject at risk is very important. Smart systems capable of monitor and record joint activity can help physicians to evaluate the health status of the joint extracting useful musculoskeletal parameter from the data acquired. In this way, the physician can compare the parameter of his patient with the reference value and can make an accurate diagnosis about the joint mobility status. [4]

Sensors used to create the device depends on the type of joint parameter it has to detect and also on other factors related to performance, cost, calibration, and service of the entire system. In general, the main focus on developing the joint monitoring system is to make the system simple, easy-to-use, cost-effective, non-invasive, wearable and with wireless communications. These characteristics are essential to use the system in real-time to collect data during the daily activities of the patients.

It is possible to investigate the health status of a joint measuring the range of motion, the joint angle and the posture of the joint during the movements. Therefore, a joint monitoring system has to record the activity of the joint in the form of meaningful data for the physicians such as angle, range of motion (ROM) and orientation. Techniques used to track the mechanics of joint during activities can be categorized based on the following three key parameters:

- **Joint angle:** each movable joint has a physiological joint angle range for specific activity or motion that depends on sex, age and other parameters of

the subject. It decreases with aging but also due to injuries or other musculoskeletal disorders. Most joint angles measurement devices were mechanical or electromechanical goniometers based on resistive potentiometers or strain gauges. They had the disadvantages of being inflexible and of having a lower accuracy than they were replaced by optical goniometers based on optical fiber sensors. Other systems use textile-based conductive sensors or flex sensors. However, to measure joint angles are now being increasingly used the inertial measurement unit (IMU) because they have a small size, are low cost and can measure 3D angle with high precision and accuracy.

- **Joint motion:** the physiological motion of the joint describes its movement from the center of joint locations. Joint movements are flexion (bending), extension (straightening), adduction (movement towards the center of the body), abduction (movement away from the center of the body) and rotations (inward and outward movements) (Figure 2.1). The ROM of a joint is the full movement it can make considering both amplitude and direction than to measure it both angle and orientation should be known. Joint monitoring systems based on goniometers, optical fiber sensors or flex sensors cannot be used because they are capable of measuring only single-axis movements as angles, while joint monitoring systems based on 3D IMU sensors can be used because they are able of measuring the 3D motion of a joint. However, the technique usually applied is imaging or video-based tracking where the joint motion is estimated from images or videos using image processing techniques. The results obtained with it are reliable and well-established but it has the disadvantage to require a pre-equipped environment and setup that prevents using it during normal daily activities. As the knee angle, the ROM can be reduced as the consequences of some health problems or injuries.
- **Skeletal tracking:** is a technique used to build a skeletal model detecting the position of various joints on a human form. It helps to obtain human pose for different activities that can be used as a comparison to identified physical disabilities. The majority of the skeletal tracking system is based on images acquired by a single camera or a network of multiple cameras and complicated image processing techniques. Due to the complexity of this technique, new simple systems based on IMU sensors placed on different joint locations on a human body are being developed.

In joint monitoring system sensors play an essential role in key parameter detection, however, their outputs should be stored and processed to obtain the final data that can be useful for the doctor to analyze the health status of the joint.

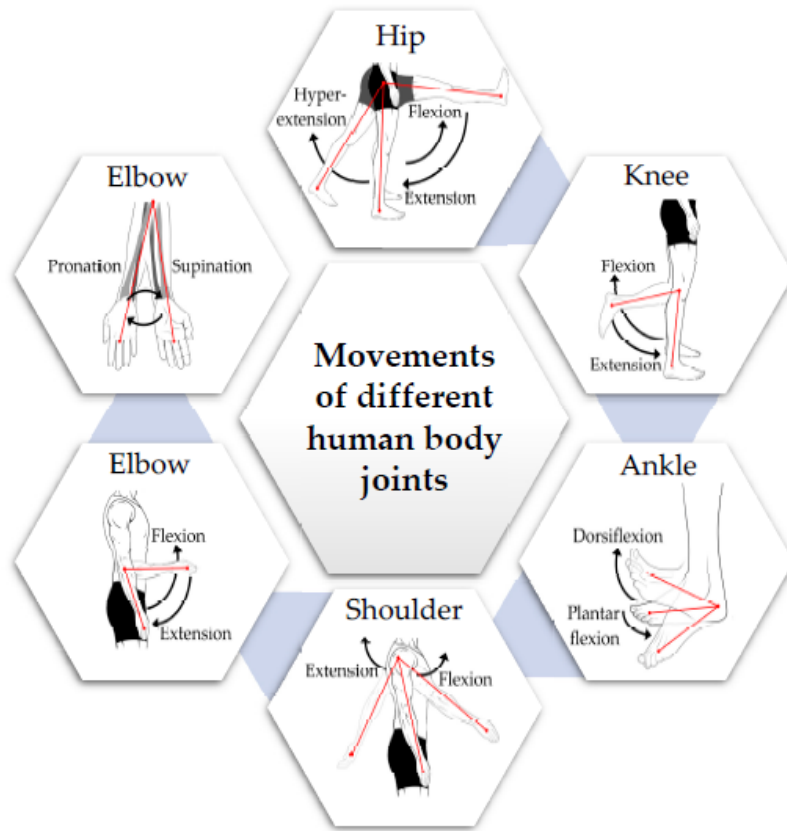


Figure 2.1: Types of joint movements. [4]

Three are the essential steps that a smart joint monitoring device must include (Figure 2.2):

1. Acquisition and processing of the data from the sensors;
2. Feature extraction and feature selection;
3. Creation of a model based on learning from the extracting features and to the expert knowledge to perform detection, prediction and decision making.

First of all the raw sensor data are acquired and pre-processed. The pre-processing is a fundamental step that consists of a first cleaning of the dataset to mitigate noise, motion artifact and sensor errors with the most suitable types of filtering techniques and if the system is composed of multiple sensors of data formatting, normalization, and synchronization. Subsequently, the feature extraction process is applied to the pre-processed data considering both the time domain and

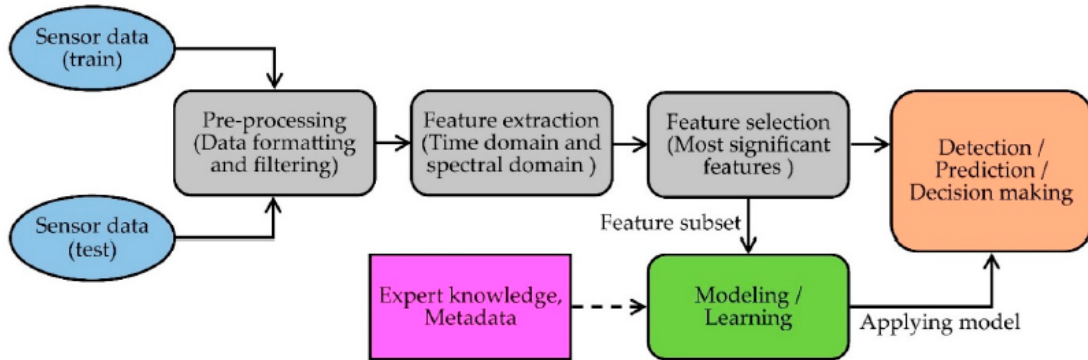


Figure 2.2: Flow diagram of a generic joint monitoring system. [4]

the frequency domain to construct the features of the dataset that are the individual measurable properties or characteristics of the data. Then, the feature selection process is used to select the most discriminative features among those extracted. At this point, the dataset is cleaned for the second time with a proper analysis method to make sense of the data and to retrieve meaningful information. The last step is the construction of the machine learning model based on the dataset obtained and expert knowledge. The type of model used depends on the type of the problem it has to solve: for classification and regression problems are used supervised algorithm, for clustering problems are used unsupervised algorithms. The first ones learning to classify or predict the data both from the input data they received and their outputs, the second ones learning to associate each data to a certain group that they created from the characteristics and patterns of the input data.

2.1.1 Optical fiber sensors

A fiber optic sensor uses fiber optic technology as a transducer or as a means of conveying information. The optical fibers are made of glass or polymeric materials that allow the conduction of light inside them. The outermost part of a fiber optic is called coating. This is a protective sheath that allows isolating the fiber from disturbing factors. The innermost part of the fiber, the core, is the area where the light wave propagation takes place. This area is surrounded by cladding. The core is characterized by a refractive index slightly greater than that of the cladding so as to be able to guide the rays inside. In Figure 2.3 is shown the general scheme of an optical fiber and how these are generally organized inside a normal cable. Generally, the light wave used in the optical fibers is in the infrared band and therefore with wavelengths between 1300 and 1600nm.

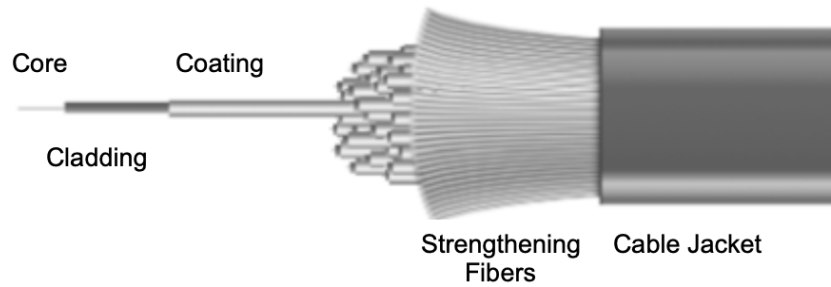


Figure 2.3: Schematic of an optical fiber. [8]

The success of fiber optics is due to the possibility, taking advantage of different characteristics of the propagation of the light beam, to measure and monitor different types of quantities such as strain, temperature, pressure, current/voltage, rotation, vibration, torsion, displacement, etc. The main advantages of these types of sensors are:

- the very low invasiveness required for the measurements;
- immunity to electromagnetic disturbances;
- no power supply in the measuring zone;
- measures implemented in space;
- a long time of life;
- high chemical and mechanical stability;
- small space occupy and light weight;
- compatible with biomedical sterilization techniques.

In the biomechanical field, fiber optics are becoming an increasingly effective alternative to make wearable devices to monitor joint angles, for example, the knee (Figure 2.4). In this type of application, the optical fiber is used as an optical strain gauge in order to evaluate the angular variations. This sensor exploits the correlation between the elastic deformation and the variation in the propagation of light of the fiber, using a Bragg grating structure.

A Bragg fiber-optic grid (FBG) is a periodic variation of the refractive index of the core of a fiber segment that allows reflection only of certain wavelengths, transmitting all the others. The operating mechanism is schematized in Figure

2.5. A fiber deformation causes a variation of the Bragg grid pitch and thus the wavelength of the reflected wave. The distributed change in the refractive index of the fiber core is achieved using photosensitive fibers.

Using this principle, the fiber optic sensors used for joint monitoring, provide a voltage output proportional to the variation of the wavelength of the reflected wave and thus to the physical deformation of the fiber. The wavelength reflected by the Bragg grating also varies with temperature. This, in the biomechanical field, is not a problem because the variation of temperature is not such to generate a disturbance in the measurement of the joint angles.

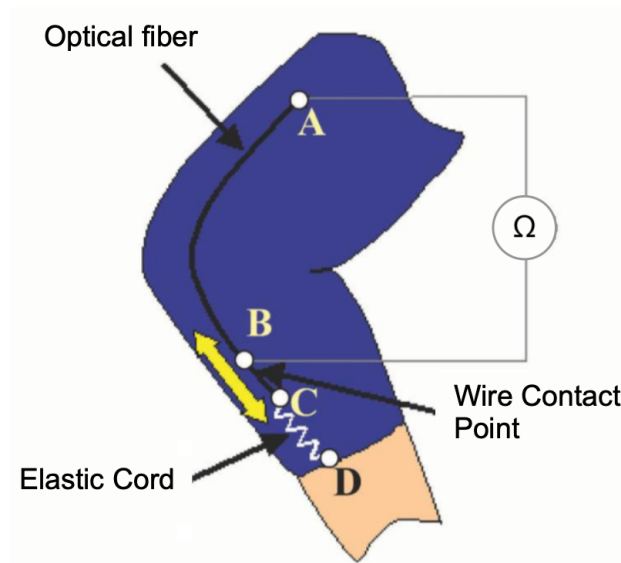


Figure 2.4: Knee monitoring using optical fiber. [9]

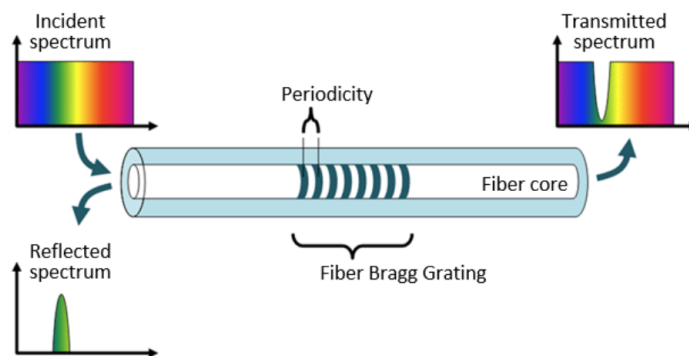


Figure 2.5: A Optical Fiber Bragg grating structure. [10]

2.1.2 Vicron motion capture system

The most widely used technology, in the biomedical field, for the instrumental analysis of motion is the Vicron optoelectronic system. This is an indoor system that, through the use of a certain number of cameras, can reconstruct the trend in time of the position taken by the markers placed on the subject to be analyzed. The number of cameras depends on the size of the analysis area. Vicron cameras work in the infrared field (wavelength between 780nm and 820nm). These record the reflections generated by the markers, which are usually spheres or semi-spheres (0.8-1.6cm in diameter) covered with reflector material. The markers are placed on the anatomical landmarks of the area that needs to be studied.

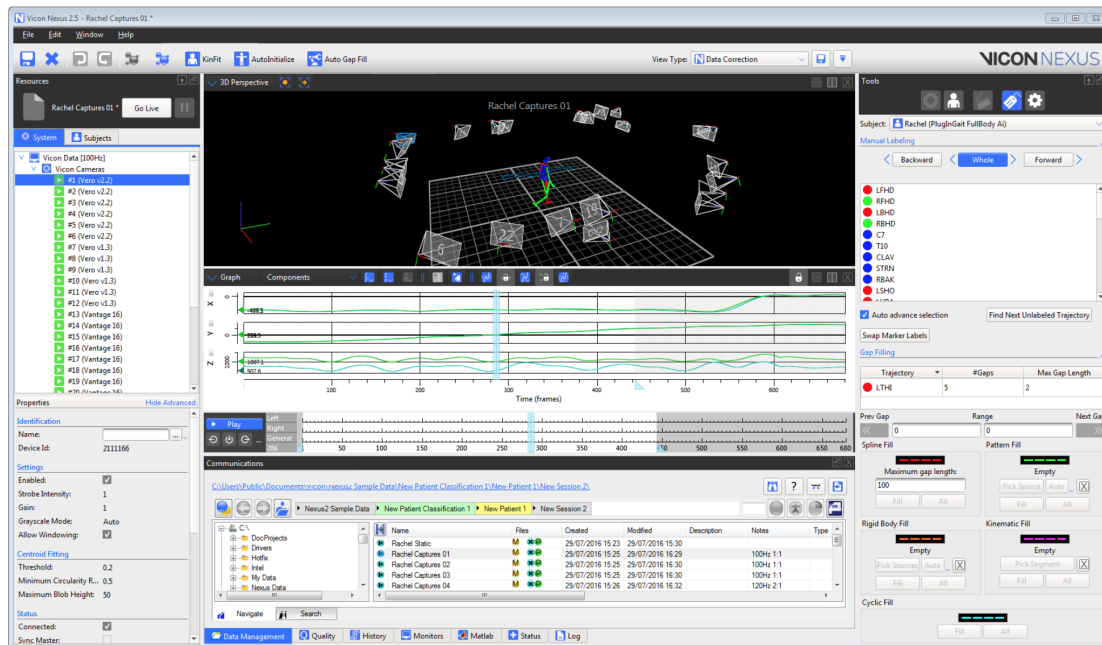


Figure 2.6: Vicron Nexus 2.0 main panel. [11]

Vicon provides the Nexus 2.0 software (Figure 2.6) needed to perform both the recording and processing of data. This software is developed on three steps:

- Calibration of the optoelectronic system: the calibration phase of the cameras is essential before proceeding with the acquisition. In this step, the software reconstructs the 3D coordinates of each marker.
- Labeling and marker tracking: this second step is responsible for the recognition and labeling of the markers (partly automatic and partly manual). The

tracking consists instead in the reconstruction of the trajectory between one frame and the successive one.

- **Data processing and modeling:** in this last step, the 3D reconstruction of the subject is realized. In this way, the kinematic variables of interest, joint angles, velocities and accelerations of the body segments can be measured.

2.1.3 Random forest

Random Forest ([12],[13]) is a supervised learning algorithm mostly used for classification and regression. It is based on an ensemble model that uses the decisional tree as an individual model and the bagging method.

- **Decisional Trees:** the decision tree is a very intuitive classifier type. The classification may be represented in terms of test sequence involving one or more attributes. In graphical terms, this classifier can be schematized as in Figure 2.7.

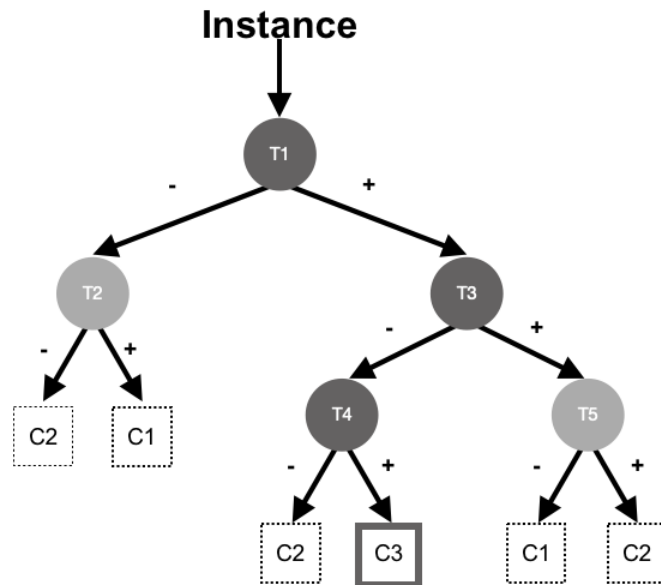


Figure 2.7: Decision Tree generic structure.

The path followed is the classification of the object. Each circle (node) indicates a test carried out on one or more attributes. Depending on the outcome, it is possible to follow a certain path in the chart (branch). So starting from the instance, the path depends on the test results. The classification ends in

a square (leaf) that indicates the class of the instance. Each node has an attribute but the number of paths that can be followed depends on the number of values that the attribute can take. To determine the class, it is not always necessary to analyze all the attributes of the element.

One of the most used methods to realize a decision tree uses a top-down approach (from the instant to the leaves of the decision tree). In this case, the classes within the training set are analyzed. If all the elements of the training set belong to the same class it is not necessary to do tests and there will be only a leaf with that class. Generally, however, the training set has several classes and therefore the easiest way to proceed is to test each attribute. Time by time, the most informative attribute is selected and the tests are carried out, to generate several possible paths equal to the number of possible values that can assume that attribute. Once the path is identified, it is important to understand if all the elements that have the same value of that attribute belong to the same class. In this case, a leaf is created. Otherwise, another attribute will be considered and proceed iteratively.

- **Bagging:** the bootstrap aggregation (bagging) is a simple and very powerful ensemble method. An ensemble method is a technique that combines predictions of multiple machine learning algorithms to make more accurate predictions than any single model. So base-learned or individual classifiers are trained with different training set bootstraps and the output with majority voting is selected.

This technique is effective if the learned base is very unstable, for example in the case of decision trees that depend very much on the training set (overfitting); different data sets are provided to each classifier and so, different decision trees will be generated. In this way, very different classifiers will be obtained to obtain a more correct classification. These different datasets are generated by resampling the initial dataset. So, for this reason, decision trees are excellent candidates for ensemble approaches.

Then, the Random Forest takes advantage of a set of decision trees (Forest), promoting the diversity of classifiers by increasing the level of randomness in the generation of decision trees (Random). Each tree, inside a Random Forest, is made and trained from a random subset of the original training set data. For each node, the absolute best attribute is no longer selected, but the best attribute is selected from a random set of attributes. Random is a factor that aims to increase diversity and decrease the correlation between the various decision trees. The final result returned by Random Forest is the average of the results returned by the different

trees in the case of a regression, or the class returned by the largest number of trees in the case of classification. An example of the graphical structure of the Random Forest is shown in Figure 2.8.

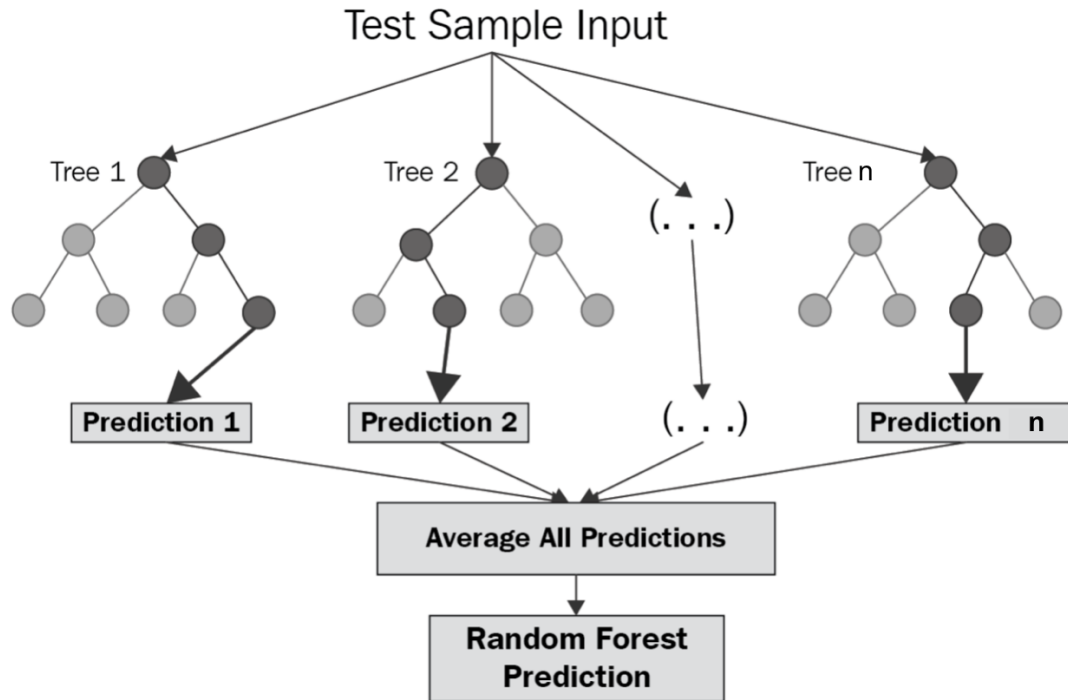


Figure 2.8: Random Forest generic structure [14]

2.1.4 Long short-term memory

A long short-term memory network (LSTM) [15] is a type of recurrent neural network (RNN) used in deep learning. LSTMs are used more in learning and classifying long data sequences. This type of network manages to consider long-term data dependencies.

The classic RNN networks are trained using time backpropagation. This causes the problem of the vanishing gradients: the information relative to previous phases decays. So short-term parameters are considered more. The reverse problem (exploding gradients) can also occur, causing the drastic growth of the error.

LSTM can overcome the problems of the vanishing, or exploding, gradients by using intermediate states to selectively store only useful information and forgetting relevant information. To do this, this type of structure uses feedback connections. An LSTM network consists of cells (LSTM blocks) chained together.

The architecture of a generic block of LSTM, shown in Figure 2.9, is typically composed of:

- **Cell state (c_t):** this is the output state of the cell;
- **Hidden state (h_t):** this acts as working memory and is similar to the latent state of RNN structures;
- **Input data (x_t):** new input data of the LSTM block;
- **Input gate (i):** defines the measurement of how a new value flows into the cell;
- **Memory cell (g):** this block handles the current memory of the cell, which will be propagated at the next instant of time ;
- **Forget gate (f):** this element is not present in traditional RNN. This serves to implement the reset function of the cell as it determines the extent by which the current value remains in the cell;
- **Output gate (o):** defines how much the value will be considered to calculate the output state of the LSTM block.

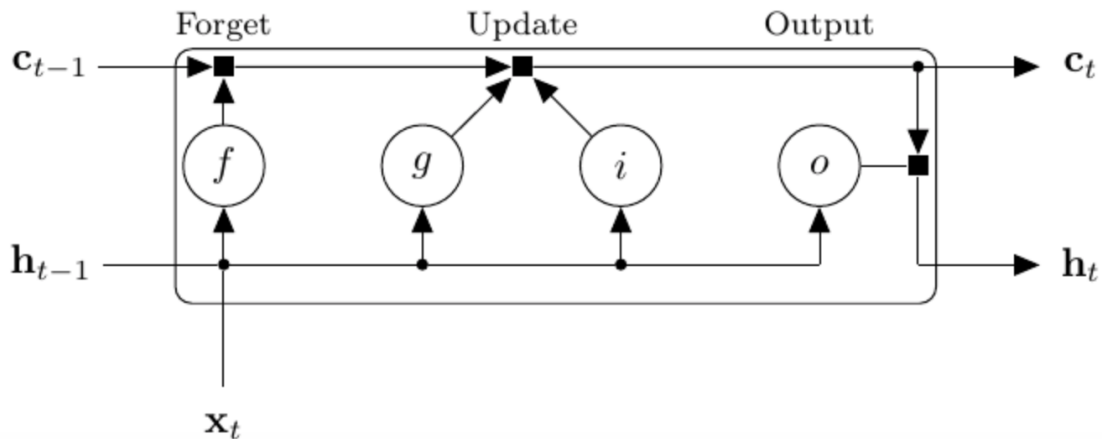


Figure 2.9: Long Short-Term Memory generic block structure [16]

A gate performs a series of matrix operations. Its state is managed by sigmoidal functions in the range $[0, 1]$, where 0 indicates inhibition and 1 the activation. Each gate has its weight matrix which must be trained to determine the working mode. In conclusion, the LSTM cell works like a mini neural network.

The LSTM network is composed by cascading several blocks, as shown in the Figure 3.13. This diagram shows the flow of a series of X data with C channels of length S within an LSTM network. The first block of the network uses only the initial data to determine the output and to generate the hidden state data. The block at time t , instead, uses both current state and current data to calculate the output. At each time pass, new information is added or removed based on the gates of the current level.

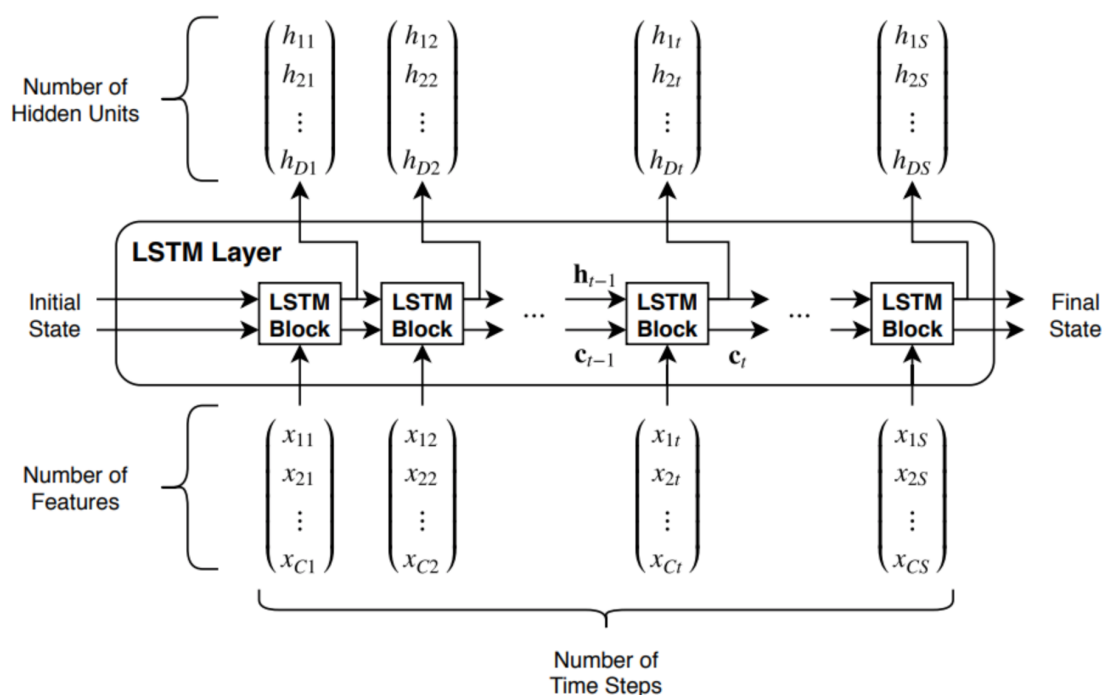


Figure 2.10: Long Short-Term Memory generic structure [16]

2.2 Mitsui's prototype

In this thesis, a joint monitoring system prototype developed by Mitsui Chemicals has been tested. The purpose of the thesis is to evaluate the performance of Mitsui's optical fiber sensor measuring knee flexion-extension angular displacement during ambulation. Vicon Motion Capture system is employed during data collection to record the output voltage of the sensor and to extract the knee angle used as references.

Mitsui Chemicals prototype is a knee sleeve with five optical fiber sensors integrated inside tight pockets. The sensors are positioned medially, laterally, inside-medially, inside-laterally than the knee and above the patella, each one of this is associated with one output channel from 1 to 5 respectively (Figure 2.11). Each optical fiber sensor is connected through a USB connector to the Mitsui box (Figure 2.12) used to drive the voltage output of the sensors to the Vicon Motion Capture system.



Figure 2.11: (a) Position and number of channel of the sensors integrated into the Mitsui Chemicals prototype; (b) Mitsui Chemicals prototype.



Figure 2.12: Mitsui box.

It is assumed that the output of multiple sensors positioned around the knee gives more information about the knee angular displacement, however, from a biomechanical point of view, the information gave by the sensors positioned medially, laterally and above the patella is similar and also the one gave by sensors positioned inside-medially and inside-laterally. During the stance phase of the gait cycle, the first group of sensors is stretched and the second group is bent, vice-versa, during the swing phase of the gait cycle the first group of the sensor is bent and the second group is stretched. As a consequence, voltage outputs of the first group of the sensors have a decrease during the swing phase, whereas, the second group has a decrease during the stance phase (Figure 2.13).

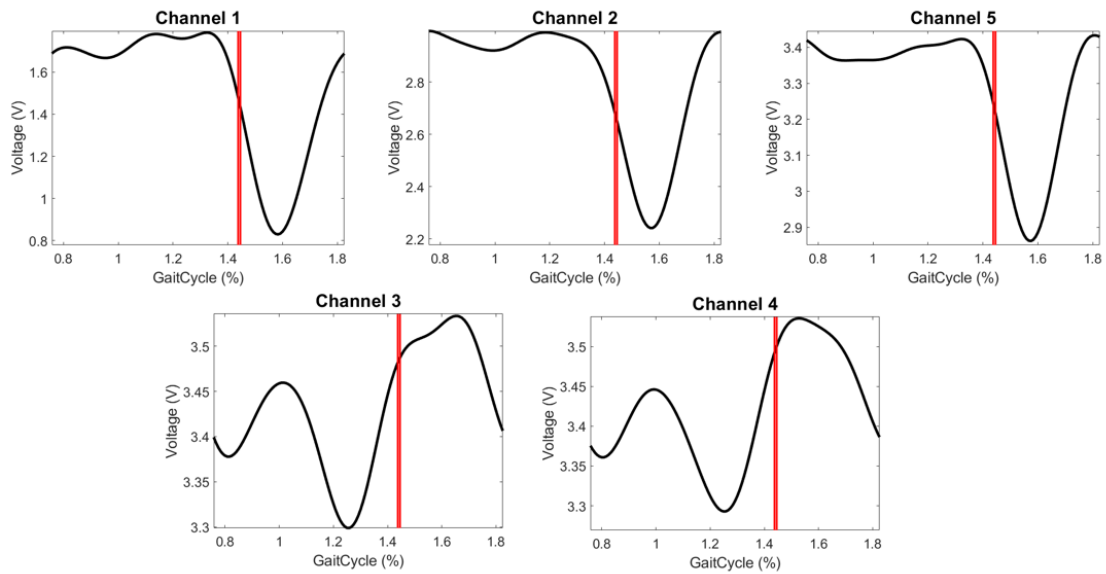


Figure 2.13: Example of the voltage output of the five sensors considering only one gait cycle. The vertical red line represents the toe-off event, before that there is the stance phase of the gait cycle and after that there is the swing phase of the gait cycle.

Chapter 3

Materials and Methods

3.1 Data collection

The data collection protocol of this thesis is the same used for the previous versions of the Mitsui prototype. It consists of walking on a treadmill at different speeds while the output of the sensors and the motion of the subject are recorded simultaneously by the Vicon motion capture system. Using the position of the markers recorded by the Vicon system is possible to extract the knee angle during the ambulation and utilized it as a reference to evaluate the knee angle that will be predicted with the voltage output of the sensors.

Twenty healthy subjects are involved in the data collection. First of all, demographic information such as age, mass, and height of the subjects are recorded, then the self-selected (SS) walking speed of each subject is evaluated. To do this, the subject gets on the treadmill and the speed is changed to find the SS speed without permitting him to know the speed value. Starting from 0 km/h the speed is increased and when the subject thinks the one reached is his normal one to walk the first speed estimate is founded. The speed continues to be increased until to reach a fast walking and then start to be decreased. For the second time, the subject has to say when he thinks his normal speed is reached to find the second speed estimate. The two estimates are averaged and the value of the SS speed is the closest one that divides by two is pair. The SS speed is called the normal speed, the slow speed is the SS speed minus its 50% and the fast speed is the SS speed plus its 50%. (Table 3.1)

Table 3.1: Subjects involved in data collection.

Subject	Age	Sex	Height (m)	Mass (kg)	Normal speed (km/h)	Slow speed (km/h)	Fast speed (km/h)
1	32	M	1.8	76	4	2	6
2	24	F	1.7	54	4.4	2.2	6.6
3	30	F	1.66	68	4	2	6
4	24	M	1.74	68	4.4	2.2	6.6
5	24	M	1.93	95	4.4	2.2	6.6
6	33	M	1.93	92	4	2	6
7	28	F	1.63	64	4	2	6
8	30	M	1.83	78	4	2	6
9	26	M	1.78	83	4.4	2.2	6.6
10	25	F	1.69	65	4	2	6
11	25	M	1.76	69	4.8	2.4	7.2
12	38	M	1.80	91	3.6	1.8	5.4
13	26	M	1.81	75	4	2	6
14	25	M	1.80	74	4.8	2.4	7.2
15	25	M	1.80	84	3.6	1.8	5.4
16	23	F	1.77	58	4	2	6
17	25	F	1.68	57	4	2	6
18	24	M	1.75	64	4	2	6
19	24	F	1.67	53	4	2	6
20	26	F	1.60	55	4	2	6

At this point, the trials without the sleeve prototype are executed, therefore, a 19 retro-reflective lower limb marker set is positioned on the subject. The locations of the markers are (Figure 3.1):

- 4 on pelvis (2 on both left and right PSIS and ASIS);
- A cluster of 4 on thigh;
- 2 on lateral and medial knee epicondyles;
- A cluster of 4 on shank;
- 2 on lateral and medial ankle malleoli;
- 3 on shoe (1 on heel, 2 on first and fifth metatarsal heads).

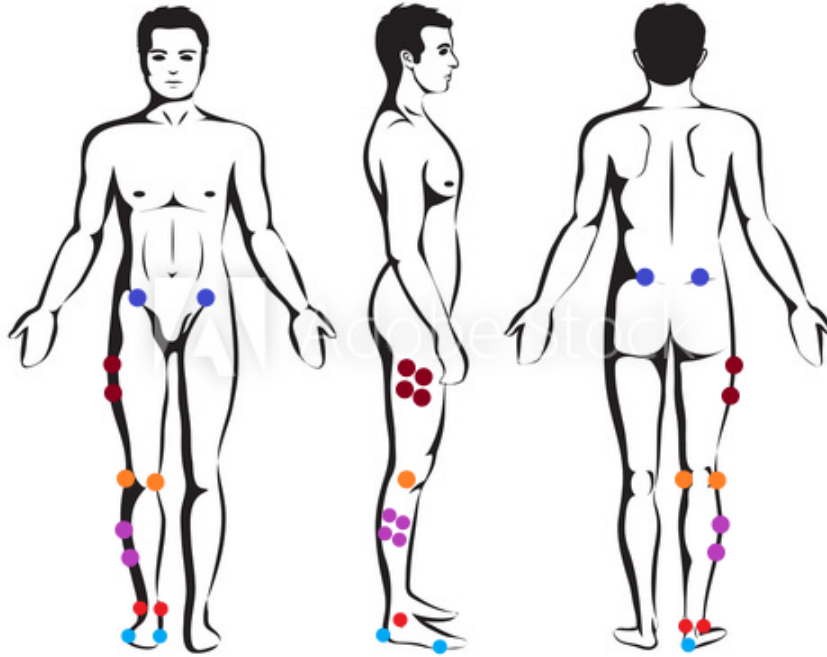


Figure 3.1: Lower limb marker set positioning.

The trials are performed with the subject on the treadmill and in order of execution are:

- Static trial: the subject remains firm for some seconds, with slightly apart legs and open arms;
- Functional hip trial: the subject perform three complete rotation anticlockwise and three clockwise with the pelvis;
- Functional knee trial: the subject perform three shallow squats;
- Knee ROM trial: the subject, holding to the treadmill, stand on one leg and execute three flexion-extension of the knee with full ROM.

Subsequently, the trials with the sleeve prototype have to be executed. The Mitsui Chemicals have realized three sizes of the prototype and for each subject, the more appropriate size must be chosen. To do this, the subject should wear the sleeve, thus the two markers on the knee, the cluster of four markers on the shank and the two markers on the ankle are detached and the shoe is removed. The subject wears the different size of the prototype and the one tighter which

doesn't create discomfort is chosen. Before to start the trials the sensors have to be calibrated with the sleeve unloaded than the subject have to take off the sleeve, the Mitsui box is connected to the Vicon system and the sensors can be calibrated at 3.5 V. At this time, the subject wear again the sleeve, the cluster of four marker on the shank is reattached on the same position and the shoe is worn, then the setup to execute the trials is ready (Figure 3.2).

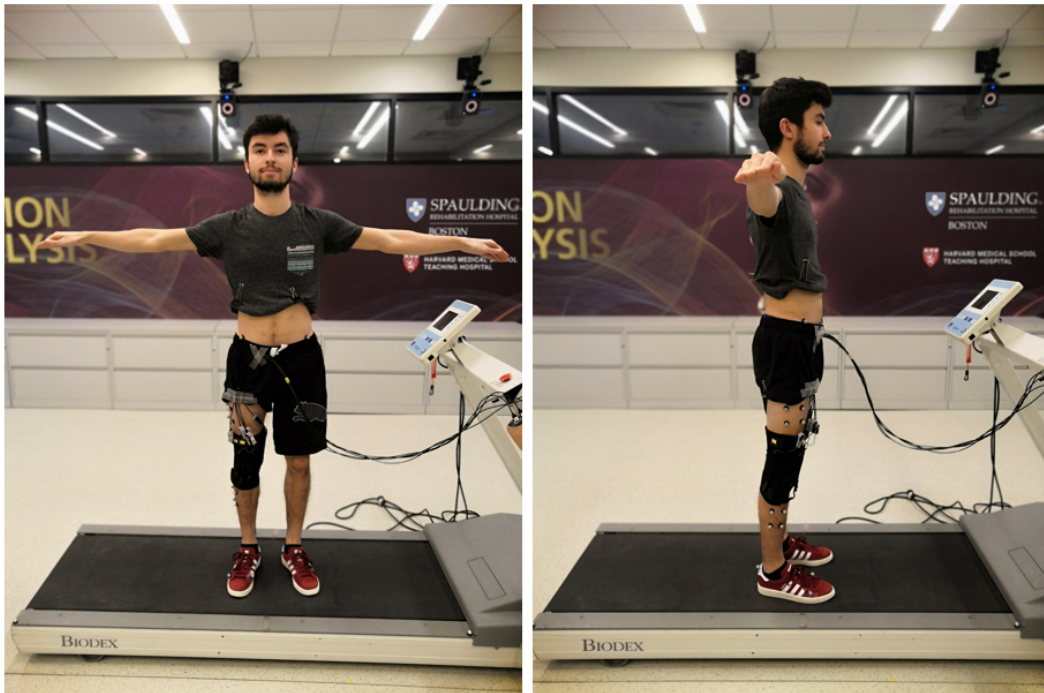


Figure 3.2: Setup of trials with Mitsui prototype.

The trials are performed, as the ones conducted without sleeve, with the subject on the treadmill and in order of execution are:

- Knee ROM trial: it's the same executed without sleeve;
- Six walking trials: the subject walks on the treadmill at different speeds for three minutes. Two trials for each speed previously detected are executed with a random order;
- Knee ROM trial: it's the same executed without sleeve;

With the last knee ROM trial, the data collection is concluded. The data recorded by the Vicon system are processed with two software, Nexus and Visual3D, and exported on a .mat file.

3.2 Data pre-processing

During the data collection, different types of trial are executed but the ones useful for the next steps are only the walking trials. For each one of these, the data saved in the .mat file are the voltage signal obtained as output of the sensors and the knee angle signal, the heel-strike events, and the toe-off events computed by the position of the marker recorded by the Vicon system (Figure 3.3). Thus, since there are six trials for each subject and twenty subjects took part in the data collection the complete dataset is composed of 120 elements, each one with five features that are the voltage signals of the five channels of the prototype and one reference that is the knee angle signal.

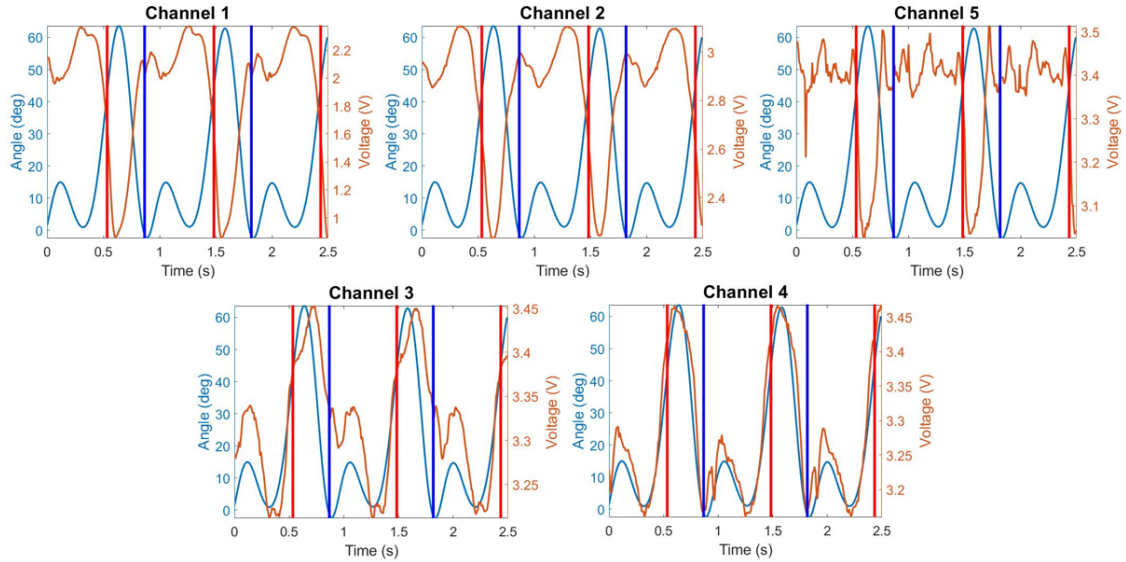


Figure 3.3: Example of the signals obtained from the data collection. The orange signal is the voltage output of the sensors, the light blue signal is the knee angle, the red lines are the heel-strike events and the blue lines are the toe-off events.

The voltage signals are the raw output of the sensors, then they have to be pre-processed before using them. First of all, they are filtered with a Butterworth low-pass filter of order 8 with a cut-off frequency of 4 Hz to remove the small fluctuations (Figure 3.4). Subsequently, a Butterworth high-pass filter of order 7 and cut-off frequency of 0.3 Hz is applied to remove the drift present in voltage signals of some subjects (Figure 3.5).

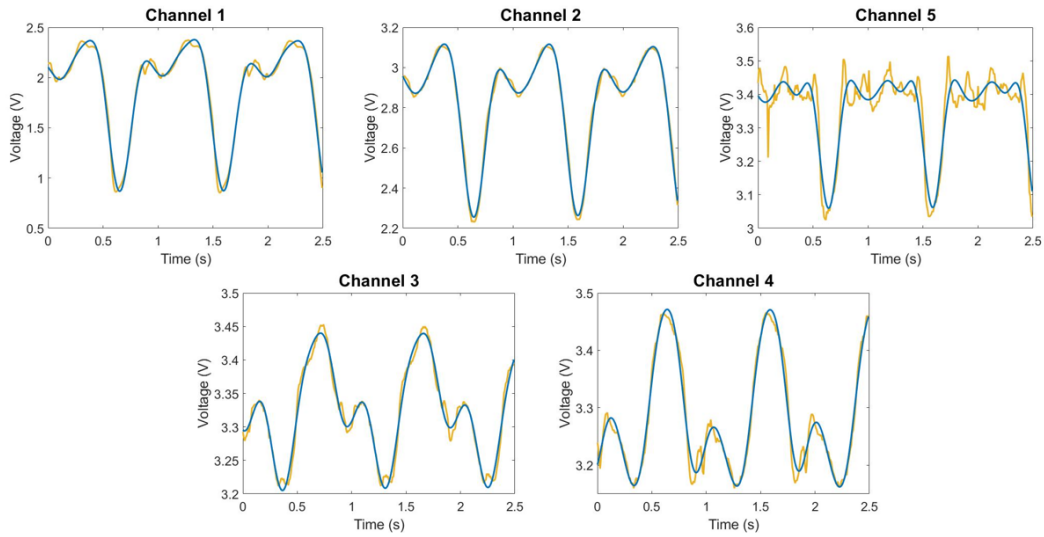


Figure 3.4: Example of the effect of the low-pass filtering. The yellow signal is the voltage signal before the low-pass filtering and the light blue signal is the voltage signal after the low-pass filtering.

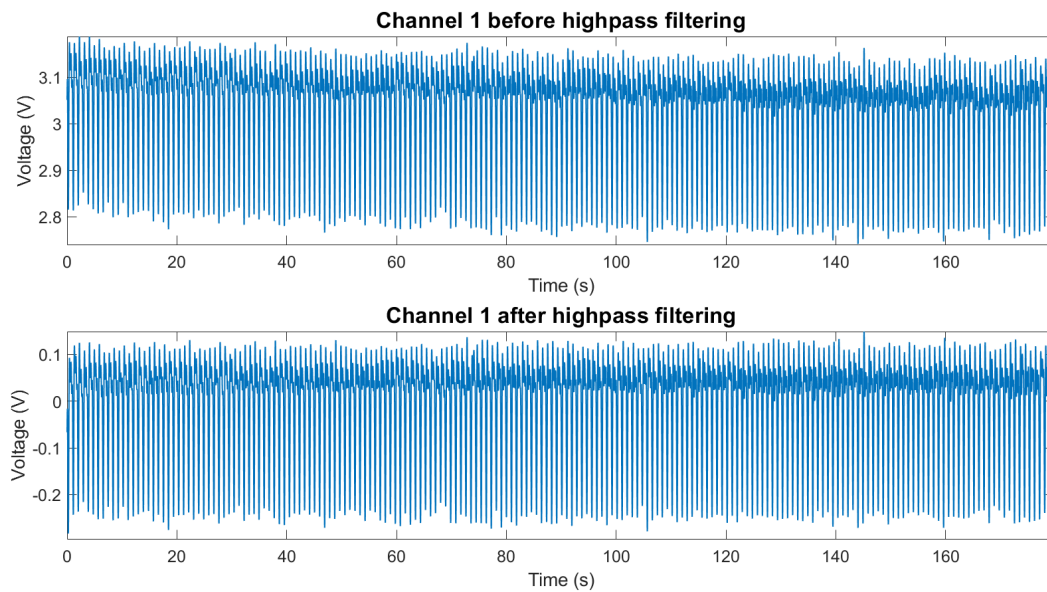


Figure 3.5: Example of the effect of the high-pass filtering. The figure on the top is the entire voltage signal of a walking trial before high-pass filtering and with the presence of the drift, the figure below is the same signal after the high-pass filtering and without drift.

In conclusion, because the range of voltage signals across the subjects sometimes is very different they have been normalized using the voltage values at 10 and 40 degrees, an angle range present in all the elements of the dataset (Figure 3.6). These values are extracted for each element averaging the value of voltage at 10 and 40 degrees of the representative gait cycles that composes them. The formula used to normalize the voltage signals is

$$signal_n = \frac{signal - signal_{10}}{signal_{40} - signal_{10}}$$

where

- $signal_n$ is the voltage signal after the normalization;
- $signal$ is the the voltage signal before the normalization;
- $signal_{10}$ is the voltage value of the signal considered at 10 degree;
- $signal_{40}$ is the voltage value of the signal considered at 40 degree.

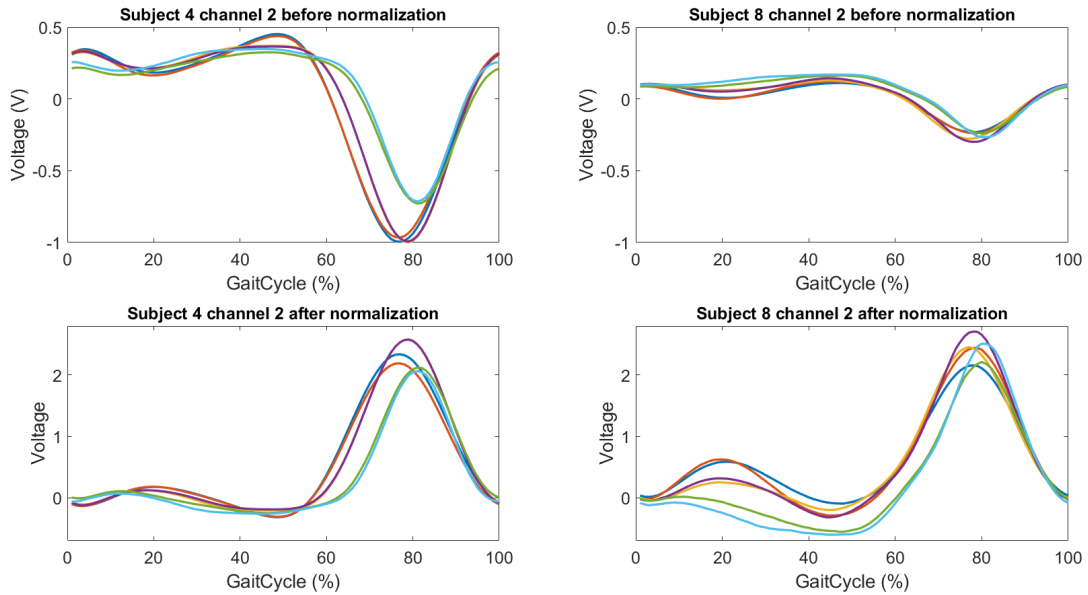


Figure 3.6: Example of the effect of the normalization in channel 2 of subject 4 and subject 8. Before the normalization, the range of the voltage signals of subject 8 is smaller than the one of subject 4, after the normalization the voltage range of the two subjects is much the same. The six signals in the four plots are the voltage signals of the six trials.

3.3 Outlier detection algorithm

During the pre-processing phase, in some voltage signals of the dataset an unusual behavior has been noticed. This consists of signals with a very different shape respect the one that was expected and signals with an excessive amplitude than that of the other signals. The voltage signals with these uncommon behaviors are called outliers and two algorithms are developed to identify them, one based on a correlation analysis to detect ambiguity in the shape and one based on an amplitude analysis to detect ambiguity in the amplitude.

3.3.1 Correlation analysis

The first type of voltage signals considered as outliers is the one with a very different shape compared to the shape expected for their channel of belonging. To find them the signals after the filtering stage are considered and are divided by channel and by the speed of the element to which they belong. Considering the dataset is composed of 120 elements and each element is composed of 5 channels, in total there are 600 voltage signals; if they are divided by 5 channels and by 3 types of speed they can be split into 15 groups, each one composed of 40 signals. (Table 3.2)

Table 3.2: Voltage signals of the dataset divided by channels and by speed.

	channel 1	channel 2	channel 3	channel 4	channel 5
fast speed	40 signals				
normal speed	40 signals				
slow speed	40 signals				

The behavior of each voltage signal of the dataset is extracted averaging the gait cycle that composes it. The average signals obtained for those of the same group are averaged to find the representative voltage signal of the group. At this point, it is assumed that signals belonging to the same group have to be correlated because the sensors used during the data collection are always the same and the subject involved in the study are healthy subjects than the output of the sensors have to be similar during the ambulation for the same channel and the same speed. Thus, the correlation coefficient (CC) between the representative voltage signals of each group and the average signals belonging to its group is computed. Those who result anticorrelated are considered outliers. (Figure 3.7)

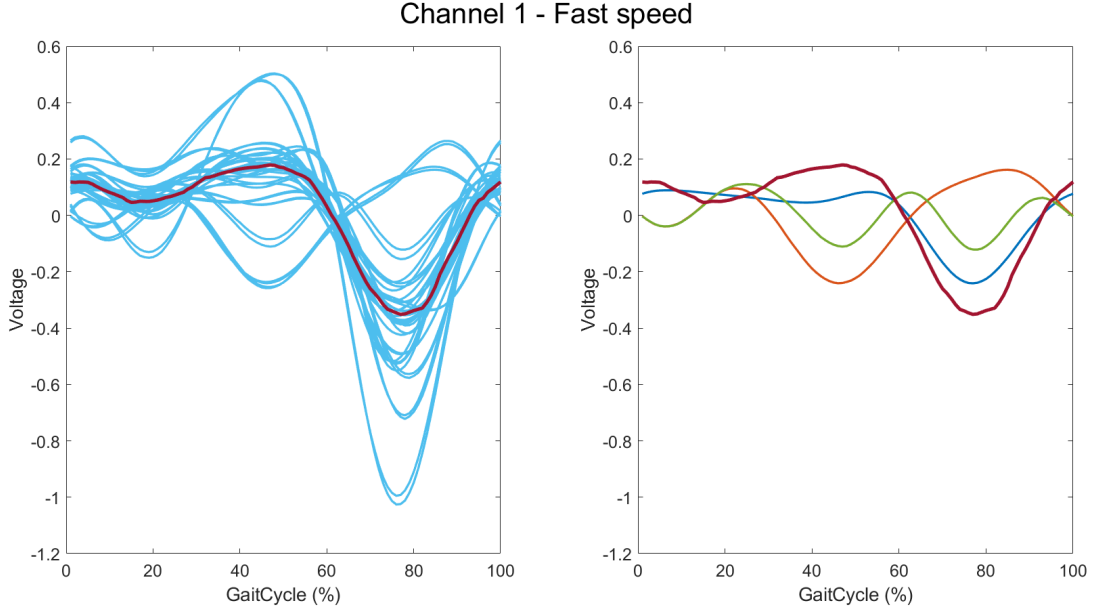


Figure 3.7: Example of correlation analysis carried out for the voltage signals belonging to the group of channel 1 and fast speed. In the figure on the left, the light blue gait cycles are the average signals extracted from all the voltage signals of this group, the red gait cycle is the representative signal of the group obtained averaging the light blue gait cycles. In the figure on the right, the red gait cycle is still the representative signal of the group, the blue gait cycle represents a high correlated signal (CC 0.96), the green gait cycle represents a medium correlated signal (CC 0.25), the orange gait cycle represents an anticorrelated signal (CC -0.75).

3.3.2 Amplitude analysis

The second type of signals considered as outliers is the one with an excessive amplitude compared to the amplitude of the other signals belonging to the same channel. The increase of amplitude is subsequent to the normalization and happens because the denominator of the formula used to normalize becomes very small since the voltage values at 10 and 40 degree are very similar. To find these type of outliers the voltage signals of the dataset are grouped by channel and, as in the correlation analysis algorithm, the behavior of each signal is extracted averaging the gait cycles which composes it. Then, the amplitude of the average signals is computed by subtracting their minimum value from their maximum value. It is assumed that the distribution of the amplitude of each channel can be considered as a normal distribution, then the signals with an amplitude which is 3 standard deviations (SD) away from the mean of the distribution are considered outliers. (Figure 3.8) (Figure 3.9)

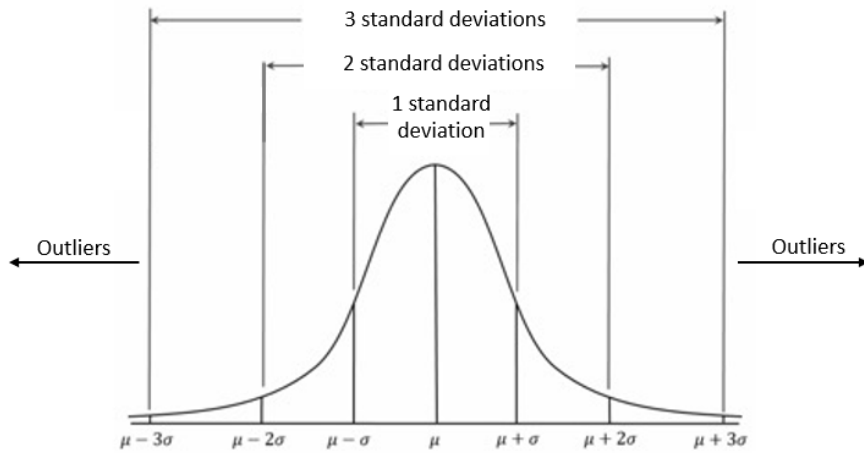


Figure 3.8: Normal distribution.

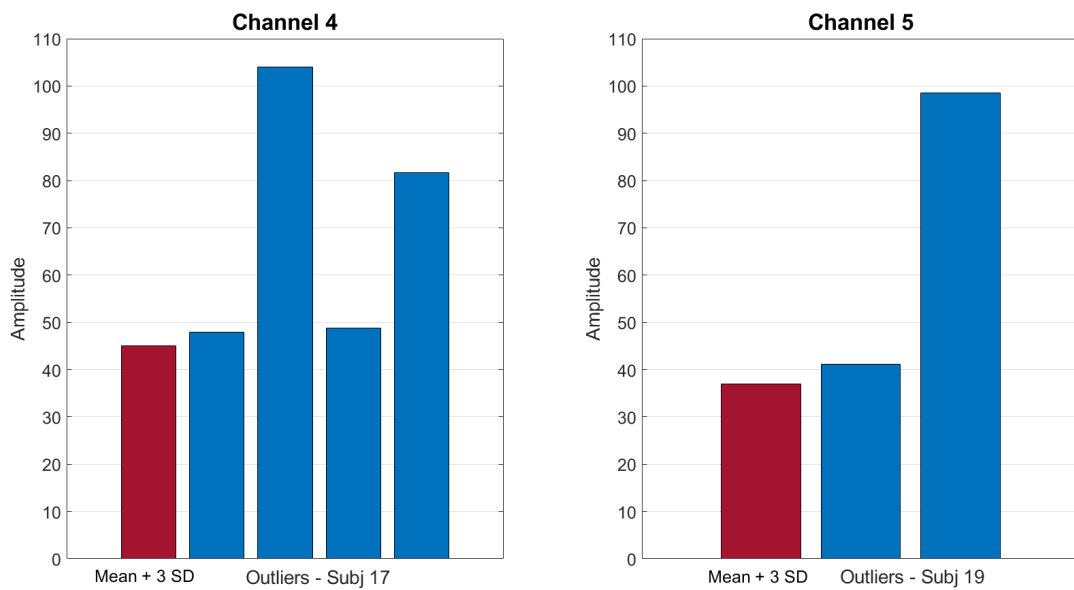


Figure 3.9: Example of the amplitude of outliers found on channel 4 and channel 5. The red bar represents the value of the mean + 3 standard deviations, the blue bars represent the amplitude of the signals identified as outliers. In this case, both the outliers of channels 4 and 5 are voltage signals of the same subject, respectively of subject 21 and subject 23.

3.4 Outlier replacement algorithm

After the detection of the outliers inside the dataset a strategy to deal with them has been developed. Since the following machine learning algorithms will use as predictors the voltage signals of the five channels of the Mitsui's prototype an algorithm to substitute the outliers with other appropriate signals is implemented.

As explained inside the section "Mitsui's prototype" of the second chapter, it is expected that voltage signals of the five channels can be divided into two sets based on the similarity of their output: the first one is composed by the channels 1, 2 and 5 and the second one by the channels 3 and 4. The first step of this algorithm is to demonstrate that the correlation among the voltage signals belonging to the same set is high enough to substitute the outliers of one channel with the voltage signals of the correlated channel. To do this, the dataset is divided into the same 15 groups described in the previous algorithm (Table 3.2). Also in this case, the behavior of all the voltage signals of the dataset is extracted averaging the gait cycles which compose them. Subsequently, the extracted signals belonging to the same group and that are not classified as outliers are averaged and a new representative voltage signal for each group is found. At this point, for each speed is computed the CC among the representative signals of the five channels (Figure 3.10).

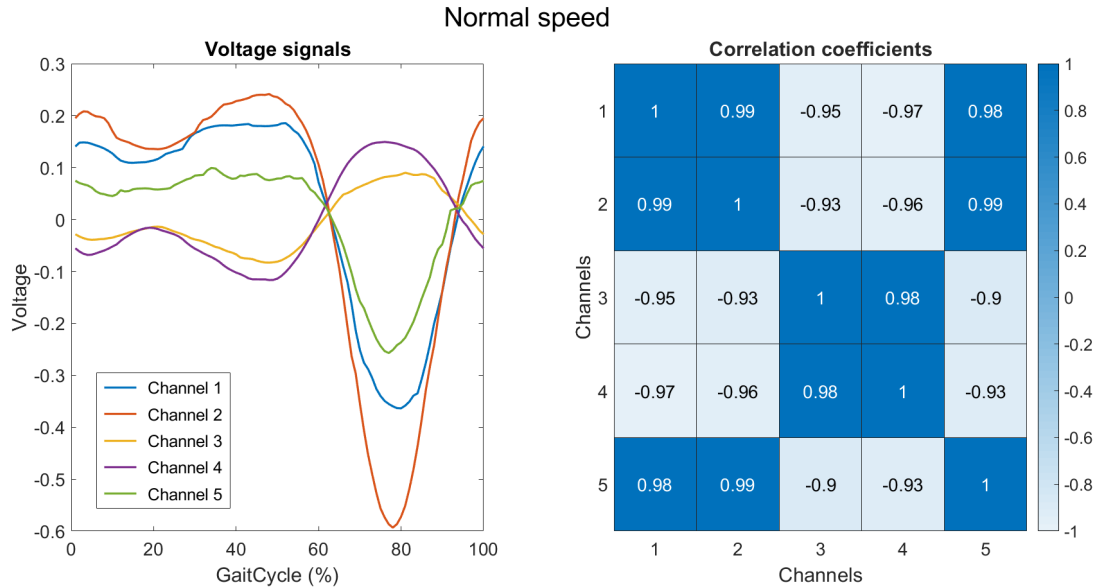


Figure 3.10: Example of the extraction of the correlation coefficients among the five channels of the normal speed. In the figure on the left, the gait cycles are the representative voltage signals for the five channels of the normal speed. In the figure on the right, there are the CC computed among the gait cycles on the figure on the left.

The CC computed separately for the three speeds are averaged and the results obtained confirmed the original assumption: the CC calculated between signals belonging to channels of the same set is very high, around 0.98 - 0.99, on the contrary, the signals belonging to channels of different sets result anticorrelated, with a CC from -0.90 to -0.96. (Figure 3.11)

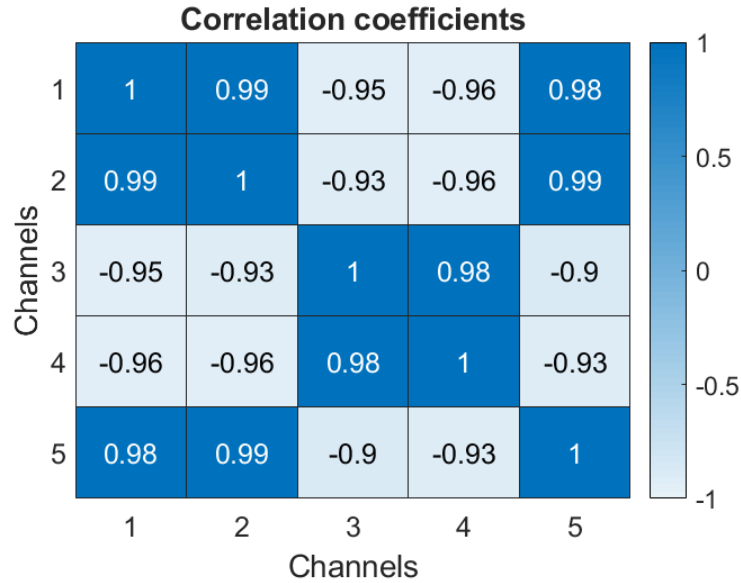


Figure 3.11: Correlation coefficients of the five channels averaged on the three speeds.

These results allow to proceed with the second step of the algorithm that is the replacement. This is carried out as listed below:

- Channel 2 does not have outliers, then, the ones of channels 1 and channel 5 are replaced with its voltage signals;
- The outliers of channel 3 are replaced with the voltage signals of channel 4 and vice-versa;
- The replacement of an outlier in one element is extended to all the other elements of the subject using for each one the respective voltage signals. This is done because also if the CCs between correlated channels are very high the signals are not completely the same. It could be confusing for the machine learning algorithm to have for the same subject different patterns inside one channel. (Figure 3.12)

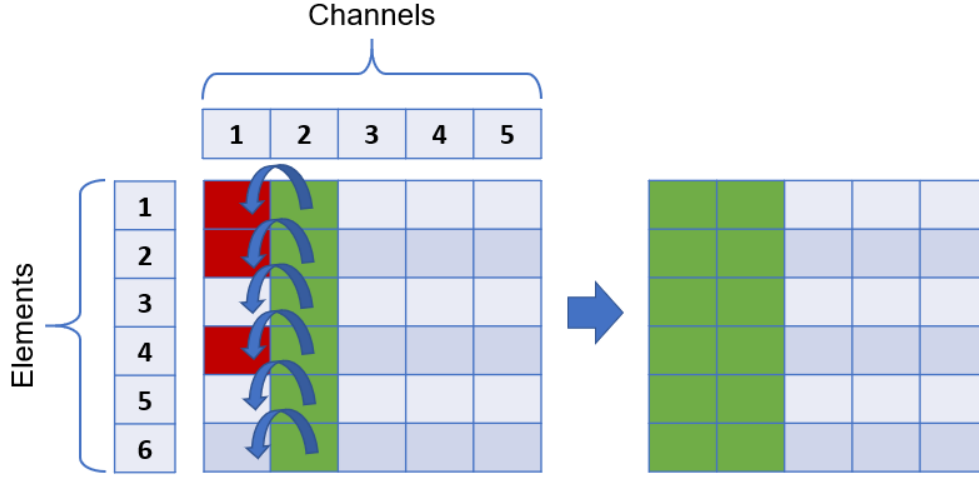


Figure 3.12: Example of outliers replacement. It is shown a subject with 3 outliers in channel 1 of the first, second and fourth element. Applying the replacement algorithm the voltage signals of channel 1 of all the elements are replaced with the voltage signals of channel 2 of the respective elements.

3.5 Machine learning algorithm

Subsequently to the outliers replacement step, it is possible to construct the machine learning model to predict the knee angle from the voltage signals of the five sensors. The model has to solve a multiple regression problem where the predictor variables are the five voltage signals and the forecast variable is the knee angle. Two types of machine learning algorithms are used: one without memory, the Random forest (RF) and one with memory, the Long short-term memory (LSTM). They are applied to the dataset with a leave-one-subject-out (LOSO) cross-validation (CV) approach. This means that for both the algorithms are created 20 models, one per subject, and for each model, all the subjects minus one are used as a training set and the excluded one is used as a test set. The performances are evaluated on each subject in terms of root-mean-squared error (RMSE).

$$RMSE = \sqrt{\sum_{i=1}^n \frac{(\hat{y}_i - y_i)^2}{n}} \quad (3.1)$$

where

- \hat{y} is the predicted value;
- y is the observed value;
- n is the number of observations.

3.5.1 Random Forest

The training set is created concatenating the five voltage signals of all the subjects minus one and the test set is created concatenating the five voltage signals of the remaining subject. The Random forest model is designed and trained with the function *TreeBagger* of Matlab.

Two parameters are tuned:

- Number of trees: 20;
- Minimum leaf size: 20.

The training is repeated with these two parameters set. The testing is executed with the function *predict* of Matlab. The predicted knee angles is obtained and is compared with the reference one to extract the RMSE value of the current subject.

3.5.2 Long short-term memory

Twenty consecutive steps are extracted from each element of the dataset. The training set is created by grouping the steps of all the subjects minus one and the test set is created by grouping the steps of the remaining subject. The steps of both the two sets are sorted by length. For each of the five channels of the two sets, the mean and the standard deviations across the steps are computed. The data are normalized with the formula

$$x_n = \frac{x - mean}{SD}$$

where

- x_n is the data after the normalization;
- x is the data before the normalization;
- $mean$ is the mean computed for one of the five channels;
- SD is the standard deviation computed for one of the five channels.

The LSTM model is designed and trained with the function *trainNetwork* of Matlab. The architecture of the LSTM network created is (Figure 3.13):

- Sequence input layer with dimension 5;
- LSTM layer with 100 hidden units;

- Fully connected layer with dimension 50;
- Dropout layer with dropout probability 0.5;
- Fully connected layer with dimension 1;
- Regression layer.

The parameters of the LSTM network chosen and tuned are:

- Number of epochs: 50;
- Mini batch size: 32;
- Learning rate: 0.001;
- Optimizer: adam.

The network is trained with these parameters set. The testing is executed with the function *predict* of Matlab using a mini-batch size of 1. The predicted knee angles is obtained and is compared with the reference one to extract the RMSE value of the current subject.

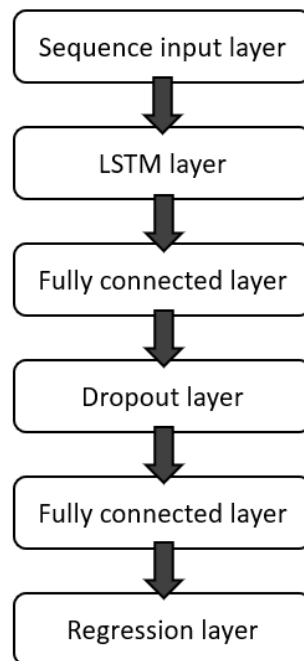


Figure 3.13: LSTM network designed.

Chapter 4

Results

4.1 Outlier detection algorithm

The outliers identified with the correlation analysis and with the amplitude analysis are shown respectively in Figure 4.4 and 4.5. The total number of outliers identified inside the dataset using both analysis techniques is 54, which is 9% of the voltage signals of the dataset (Figure 4.6). The outliers are distributed across subjects, speeds and channels respectively as shown in Figure 4.1, 4.2 and 4.3.

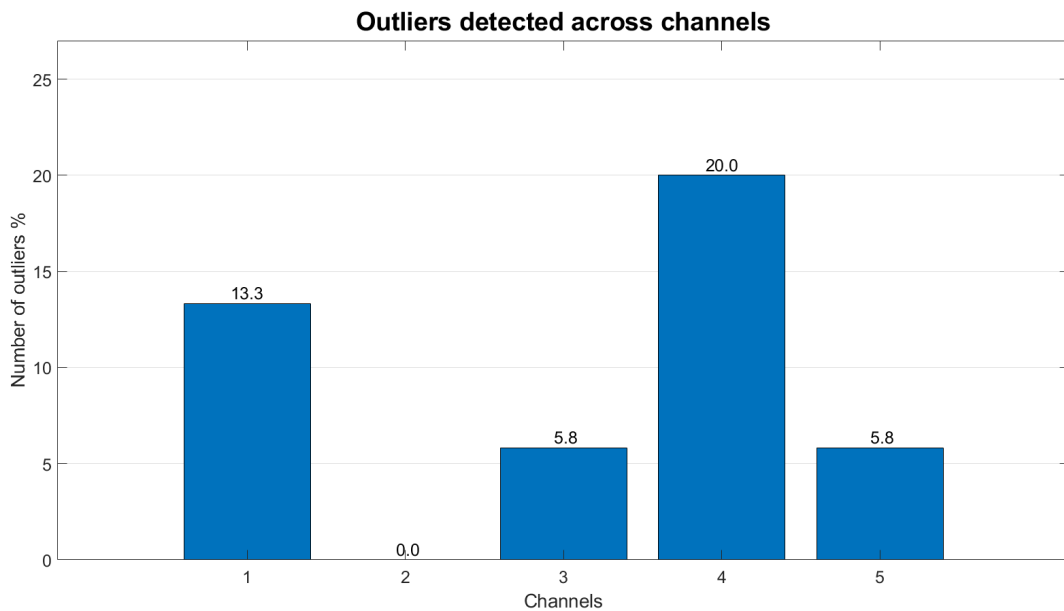


Figure 4.1: Percentage of outliers detected for each channel relative to the maximum number of voltage signals belonging to each channel, which is 120.

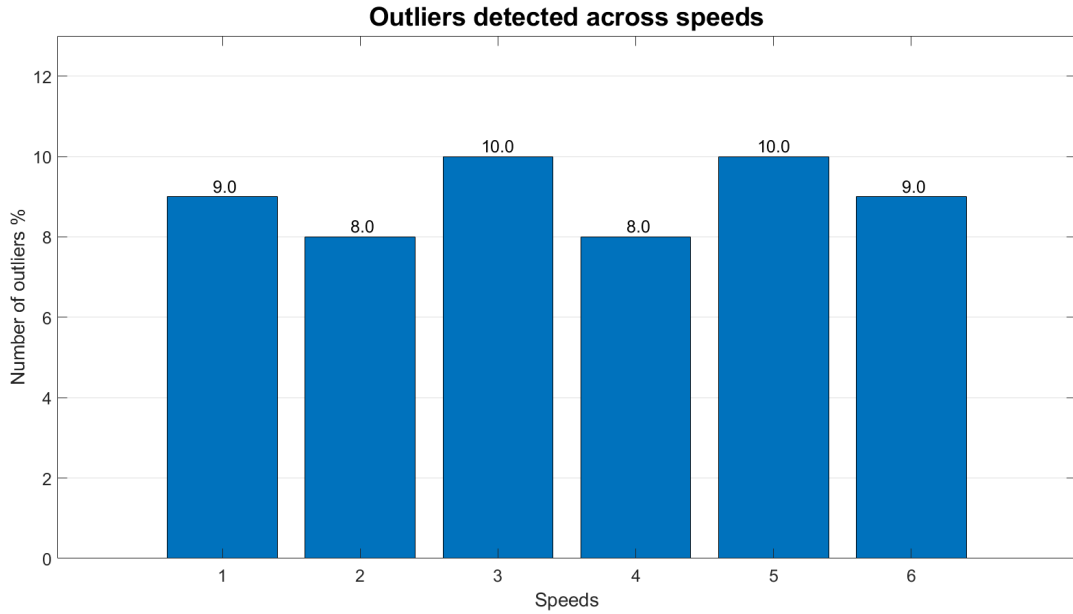


Figure 4.2: Percentage of outliers detected for each speeds relative to the maximum number of voltage signals belonging to each speed, which is 100.

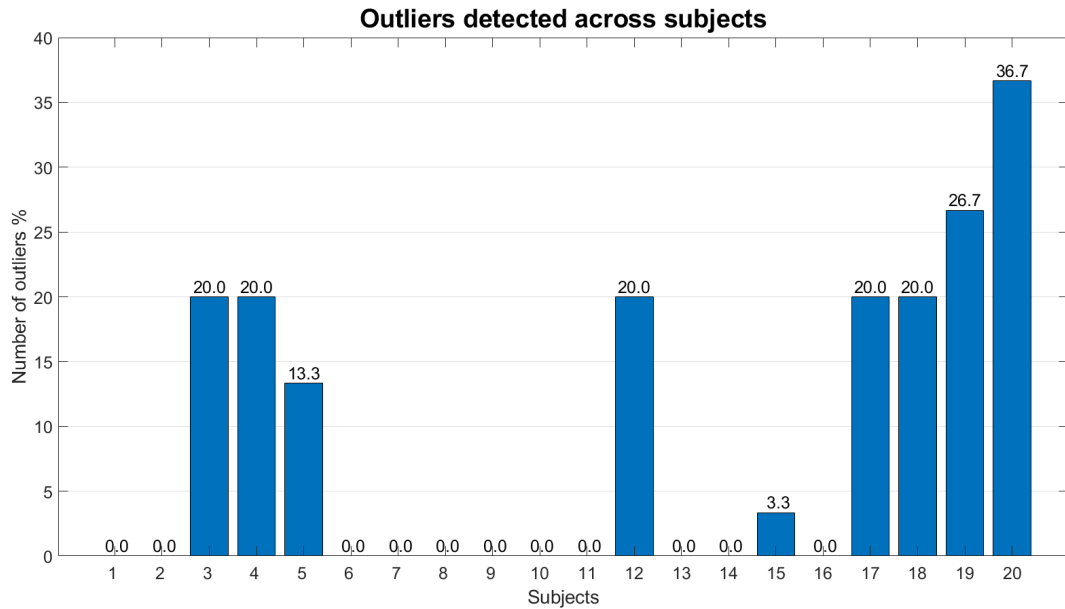


Figure 4.3: Percentage of outliers detected for each subject relative to the maximum number of voltage signals belonging to each subject, which is 30.

4.2 Outlier replacement algorithm

After the outliers replacement, the subjects with 1 or 2 outliers inside their channels will have respectively 2 or 4 of 5 equal channels (Figure 4.7). The subjects involved in the replacement are 9 of 20, of which 7 have 2 equal channels and 2 have 4 equal channels (Table 4.1).

Table 4.1: Channels replacements made across subjects

Subject	Channel outliers	Equal channels
3	ch1	[ch1,ch2]
4	ch1	[ch1,ch2]
5	ch1	[ch1,ch2]
12	ch3	[ch3,ch4]
15	ch4	[ch3,ch4]
17	ch4	[ch3,ch4]
18	ch4	[ch3,ch4]
19	ch4,ch5	[ch2,ch5],[ch3,ch4]
20	ch4,ch5	[ch2,ch5],[ch3,ch4]

4.3 Machine learning algorithm

The general results obtained in terms of RMSE for the Random forest and the LSTM are shown in the following Table 4.2. The results obtained in terms of RMSE, for each subject, are shown in Figure 4.8.

Table 4.2: RMSE

	mean (°)	SD (°)	min (°)	max (°)
RF	5.22	1.94	2.51	9.29
LSTM	4.56	1.74	2.28	8.21

4.4 Discussion

Considering the distribution of outliers identified inside the dataset it is possible to notice that:

- they are distributed differently across the channels, in particular, channel 2 is the only one without outliers and channel 4 is the one with the highest number of outliers (Figure 4.1);
- they are almost equally distributed across speeds (Figure 4.2);
- they are distributed primarily on two groups of subjects, one at the beginning of the dataset, subject 3, 4 and 5, and one at the end of the dataset, subject 17, 18, 19, and 20 (Figure 4.3). Moreover, all the subjects of the first group have an outlier in channel 1 and all the subjects of the second group have an outlier in channel 4 (Figure 4.6);

It can be deduced from these three observations that the presence of outliers is not correlated with the walking speed but with a factor involving both the subjects and the channels. Given that during the data collection different sizes of the sleeve are used and sometimes sensors are substituted due to their malfunctioning, the outliers could be related both to an inappropriate size of the sleeve or of failure relative to some specific sensors used for subjects in a row. Also, since channel 2 is the only one without outliers identified it could be considered the most robust channel.

Considering the results in terms of RMSE achieved with the two machine learning models designed it is possible to notice that:

- the averaged RMSE obtained with the LSTM is smaller than the one obtained with the RF but of only 0.66° (Table 4.2). However, looking at the resulting values of RMSE for each subject the LSTM obtains a small value of RMSE for 80% of the subjects (Figure 4.8);
- subjects with replaced channels allow obtaining both a small or large value of RMSE respect to the average RMSE. For example, subjects 3, 4 and 5 permits to achieve RMSE values comparable with the ones of subjects without channels replaced, on the contrary, subject 17 is one of the subjects with the highest value of RMSE;
- for the subjects 18, 19, and 20 the RF obtains the highest values of RMSE, instead, the LSTM gets values around the average RMSE. In particular, for

subject 20, one of the two subjects with 2 channels replaced, it achieves an RMSE value under the average RMSE;

- the subject with the highest value of RMSE is a subject without outliers and then without replaced channels.

These results confirming that a machine learning model with memory is capable to better manage the time series prediction respect to a model without memory. The fact that subjects with replaced channels permit to have a small value of RMSE means that not all the five channels are necessary to achieve a good prediction, but what it is needed is at least have two good channels between the two groups of 1, 2 and 5 and 3 and 4 (as it happens in subject 20). Having 5 good channels can lead to reaching a value of RMSE around 2-3°. The presence of subjects without outliers but with a large value of RMSE is due to the fact that they have uncommon signals in their channels that are not recognized by the outlier detection algorithms implemented.

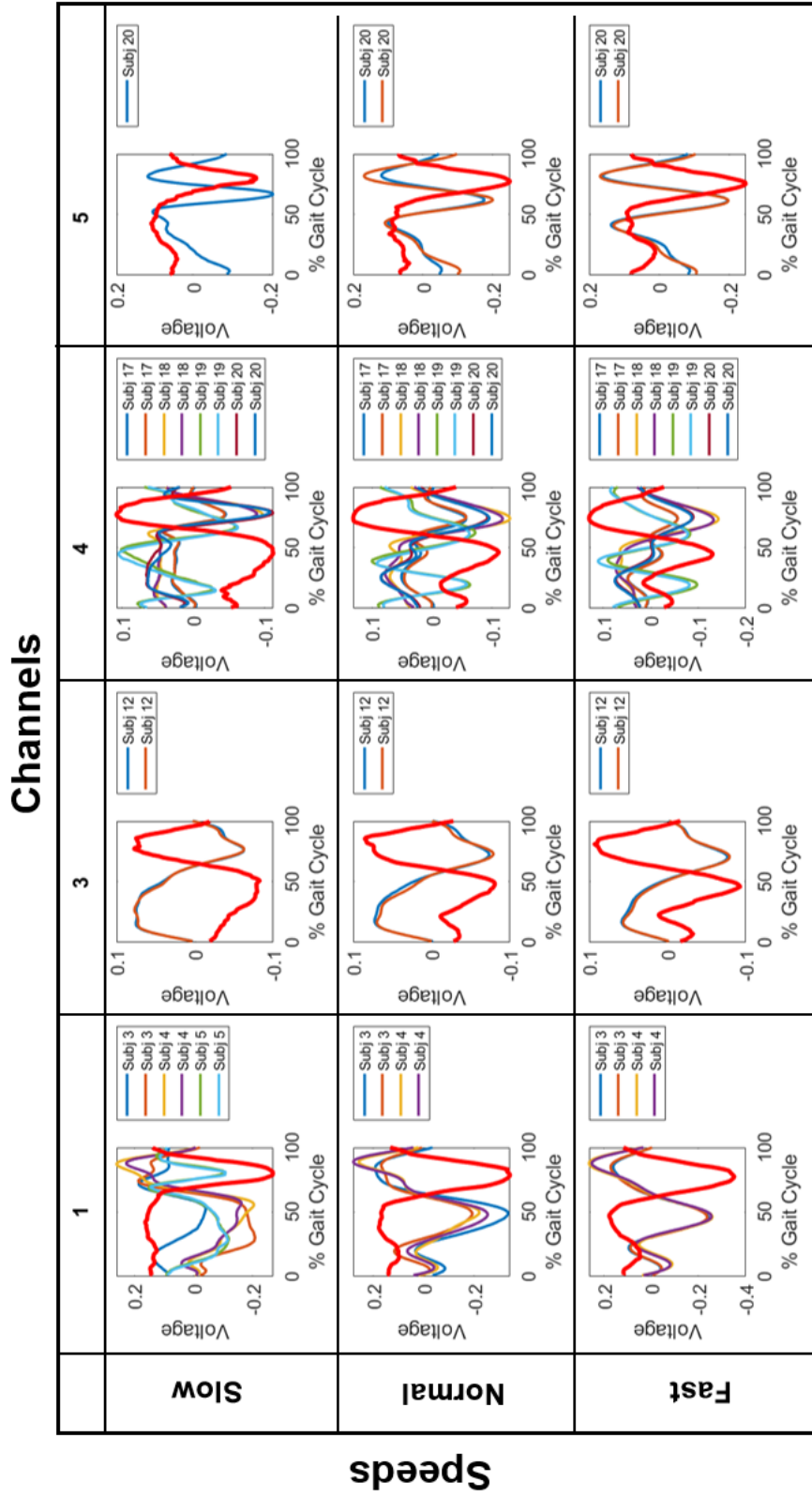


Figure 4.4: All the outliers identified with the correlation analysis algorithm are shown divided by channels and speeds. The red gait cycles present in each figure are the representative voltage signal of the group. The other colored gait cycles present in each figure are the outliers identified for the group. The subject of belonging of the outliers is reported in the legend.

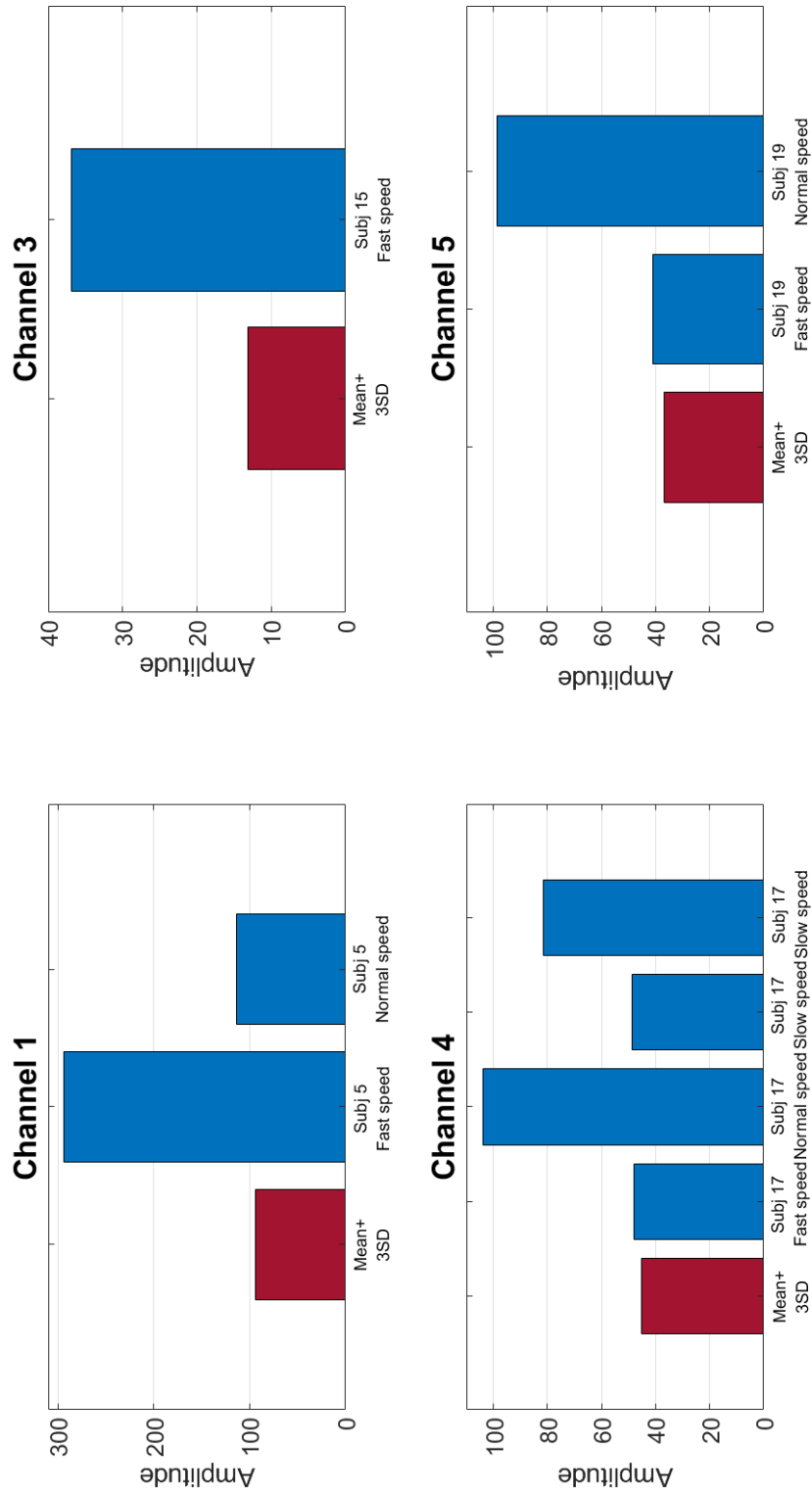


Figure 4.5: All the outliers identified with the amplitude analysis algorithm are shown divided by channels. The red bar is the amplitude beyond which a signal is considered an outlier. The blue bars are the amplitude of the outliers identified.

Total outliers detected inside the dataset																														
	Speed Slow (1)					Speed Slow (2)					Speed Normal (1)					Speed Normal (2)					Speed Fast (1)					Speed Fast (2)				
	Ch1	Ch2	Ch3	Ch4	Ch5	Ch1	Ch2	Ch3	Ch4	Ch5	Ch1	Ch2	Ch3	Ch4	Ch5	Ch1	Ch2	Ch3	Ch4	Ch5	Ch1	Ch2	Ch3	Ch4	Ch5	Ch1	Ch2	Ch3	Ch4	Ch5
Subject 1																														
Subject 2																														
Subject 3																														
Subject 4																														
Subject 5																														
Subject 6																														
Subject 7																														
Subject 8																														
Subject 9																														
Subject 10																														
Subject 11																														
Subject 12																														
Subject 13																														
Subject 14																														
Subject 15																														
Subject 16																														
Subject 17																														
Subject 18																														
Subject 19																														
Subject 20																														

Figure 4.6: The table represents the outliers detected inside the dataset by adding the ones found by the correlation analysis and the ones found by the amplitude analysis. Each red square is an outlier.

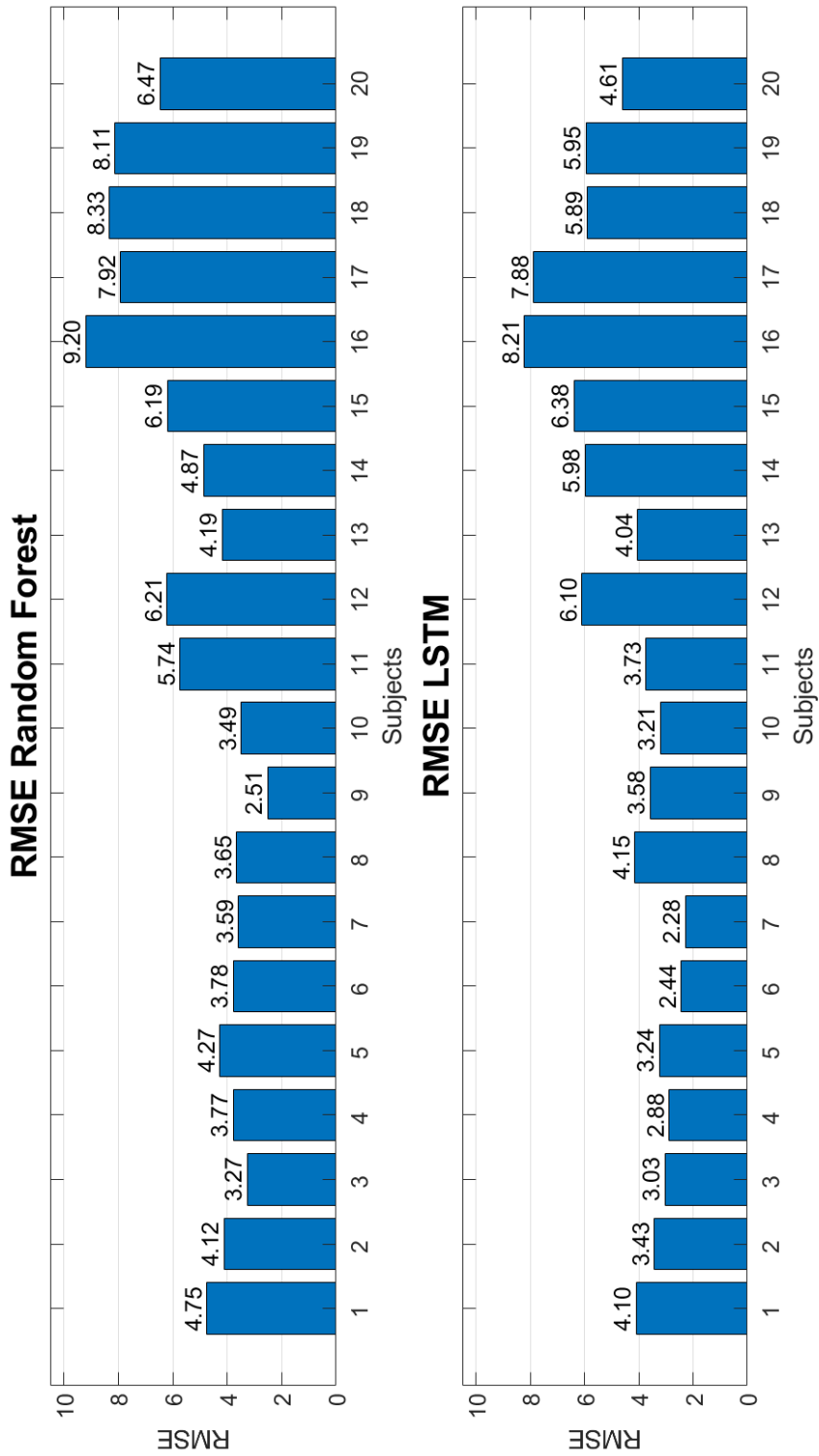


Figure 4.8: The two figures indicate the value of RMSE obtained for each subject respectively using the Random Forest model and the LSTM model.

Chapter 5

Conclusions

This thesis has aimed to demonstrate the feasibility of the use of the Mitsui's optical fiber sensors to measure the knee flexion-extension angle during ambulation. The Mitsui Chemicals has provided a sleeve prototype with five sensors integrated to collect the data. The work done for this purpose can be resumed in four steps:

- Acquisition of the data: 20 healthy subjects are involved in a data collection procedure to capture the output of the sensors and the knee angle to use as a reference;
- Analysis of the data: the data acquired are pre-processed, then two algorithms to identified and manage uncommon data considered as outliers are developed and applied;
- Knee angle prediction: two machine learning models are designed and applied to the data to predict the knee angle from the voltage output of the Mitsui sensors;
- Analysis of results: the knee angle predictions obtained from the two machine learning models are compared and evaluated in terms of RMSE.

Considering the knee angle predictions achieve it is possible to say that in general with the voltage outputs of at least two channels of the prototype it is possible to obtain good results and that using all the five channels the results are improved.

At the end of the work, some of its improvements can be suggested. The more important are lead to:

- Sensors resistance: during the data collection often happened that after using sensors for some subjects they have to be changed due to malfunctions. Then, their resistance has to be increased to use them continuously during ambulation;
- Sensors calibration: the calibration of the sensors is done with the sleeve unloaded but it would be better done it with the sleeve worn by the subject. In this way, it is possible to associate a certain angle to the same value of voltage for all the subjects and this value can be used to normalize the signals;
- Dataset enlargement: the dataset is composed of 20 subjects and some of them have reported signals with uncommon behavior respect to the general behavior of the dataset. It would be useful to record other subjects to realize a more consistent normal behavior of the voltage signals of each channel and to give to the machine learning algorithm more information to predict the knee angle;

Other improvements can be obtained using different algorithms for outliers detection and management and using different types of models to predict the knee angle.

Bibliography

- [1] A. Benjamin, “Musculoskeletal system,” 2020. "<https://www.kenhub.com/en/library/anatomy/the-musculoskeletal-system>".
- [2] Wikipedia contributors, “Human musculoskeletal system — Wikipedia, the free encyclopedia,” 2020. "https://en.wikipedia.org/w/index.php?title=Human_musculoskeletal_system&oldid=942960087".
- [3] N. Palastanga and R. Soames, *Anatomy and Human Movement, Structure and Function*, ch. 1, pp. 8–20. Elsevier, 6 ed., 2012.
- [4] A. I. Faisal, S. Majumder, T. Mondal, D. Cowan, S. Naseh, and M. J. Deen, “Monitoring methods of human body joints: State-of-the-art and research challenges,” *Sensors*, vol. 19, no. 11, 2019.
- [5] M. Hirschmann and W. Müller, “Complex function of the knee joint: the current understanding of the knee,” *Knee surgery, sports traumatology, arthroscopy : official journal of the ESSKA*, vol. 23, 05 2015.
- [6] C. Andrew, “Knee anatomy, function and common problems,” 03 2019. "<https://www.healthpages.org/anatomy-function/knee-joint-structure-function-problems/>".
- [7] Department of Research Scientific Affairs, American Academy of Orthopaedic Surgeons, “Arthritis of the knee,” 05 2014. "<https://orthoinfo.aaos.org/en/diseases--conditions/arthritis-of-the-knee/>".
- [8] H. K. Hisham", “Optical fiber sensing technology: Basics, classifications and applications,” *American Journal of Remote Sensing*, vol. 6, 02 2018.
- [9] G. M. Salim and M. A. Zawawi, “Knee joint movement monitoring device based on optical fiber bending sensor,” 2018.
- [10] Hittech, “Noria – the fiber bragg grating manufacturing solution,” 03 2019. "<https://hittech.com/nl/portfolio-posts/noria-the-fiber-bragg-grating-manufacturing-solution/>".
- [11] Vicon, “Vicon nexus user guide,” 03 2019. "<https://docs.vicon.com/display/Nexus25/PDF+downloads+for+Vicon+Nexus?preview=/50888706/50889380/Vicon%20Nexus%20User%20Guide.pdf>".

- [12] T. D. Science, "Understanding random forest," 03 2019. "<https://towardsdatascience.com/understanding-random-forest-58381e0602d2>".
- [13] Wikipedia contributors, "Random forest — Wikipedia, the free encyclopedia," 03 2020. "https://en.wikipedia.org/w/index.php?title=Random_forest&oldid=945233128".
- [14] T. D. Science, "Random forest regression," 03 2019. "<https://towardsdatascience.com/random-forest-and-its-implementation-71824ced454f>".
- [15] S. Hochreiter and J. Schmidhuber, "Long short-term memory," vol. 9, no. 8, 1997. "<https://www.bioinf.jku.at/publications/older/2604.pdf>".
- [16] MathWorks, "Long short-term memory networks," 03 2019. "<https://it.mathworks.com/help/deeplearning/ug/long-short-term-memory-networks.html>".